© 2018. Published by The Company of Biologists Ltd | Journal of Cell Science (2018) 131, jcs213736. doi:10.1242/jcs.213736

RESEARCH ARTICLE

The physiological regulation of macropinocytosis during *Dictyostelium* growth and development

Thomas D. Williams* and Robert R. Kay*

ABSTRACT

Macropinocytosis is a conserved endocytic process used by *Dictyostelium* amoebae for feeding on liquid medium. To further *Dictyostelium* as a model for macropinocytosis, we developed a high-throughput flow cytometry assay to measure macropinocytosis, and used it to identify inhibitors and investigate the physiological regulation of macropinocytosis. *Dictyostelium* has two feeding states: phagocytic and macropinocytic. When cells are switched from phagocytic growth on bacteria to liquid media, the rate of macropinocytosis slowly increases, due to increased size and frequency of macropinosomes. Upregulation is triggered by a minimal medium containing three amino acids plus glucose and likely depends on macropinocytosis itself. The presence of bacteria suppresses macropinocytosis while their product, folate, partially suppresses upregulation of macropinocytosis. Starvation, which initiates development, does not of itself suppress macropinocytosis: this can continue in isolated cells, but is shut down by a conditioned-medium factor or activation of PKA signalling. Thus macropinocytosis is a facultative ability of *Dictyostelium* cells, regulated by environmental conditions that are identified here.

This article has an associated First Person interview with the first author of the paper.

KEY WORDS: *Dictyostelium*, Macropinocytosis, Endocytosis, Flow cytometry

INTRODUCTION

Macropinocytosis, first described in the 1930s (Lewis, 1931), is a process of large-scale, non-specific fluid uptake carried out by a wide variety of cells. Actin-driven protrusions from the plasma membrane form cup-shaped circular ruffles that can be several microns in diameter. When a ruffle closes, it engulfs and delivers extracellular material to the cell interior in macropinosomes. Macropinosomes proceed through the endocytic system where their contents can be broken down by digestive enzymes and useful metabolites extracted (Buckley and King, 2017; Bloomfield and Kay, 2016; Swanson, 2008).

In the immune system, dendritic cells and macrophages use macropinocytosis to sample environmental antigens for presentation to B and T cells (Sallusto et al., 1995; Norbury et al., 1995). Certain bacteria and viruses can utilise macropinocytosis to invade host cells (Marechal et al., 2001; Nanbo et al., 2010; Hardt et al., 1998), while other bacteria stimulate macropinocytosis to promote toxin internalisation (Lukyanenko et al., 2011). Prions and neurodegenerative protein deposits also exploit macropinocytosis to invade new host cells (Magzoub et al., 2006; Fevrier et al., 2004; Münch et al., 2011; Falcon et al., 2015). Tumour cells can maintain a high rate of macropinocytosis (Lewis, 1937), with Ras-activated cancer cells obtaining a substantial part of their nutrition in this way (Commisso et al., 2013).

Considering its widespread importance, the basic biology of macropinocytosis is poorly understood. It has been studied most intensively in tissue culture cells, particularly macrophages, although genetic screens have also been performed in *Caenorhabditis elegans* (Fares and Greenwald, 2001) and *Dictyostelium discoideum* (Bacon et al., 1994). *Dictyostelium* in particular has great potential as a model because of the high constitutive rate of macropinocytosis maintained by cells in the right circumstances, and because the evolutionary distance from mammalian cells should allow conserved core features to be discerned.

The high rate of macropinocytosis by standard axenic strains of *Dictyostelium* used in the laboratory is due to deletion of the RasGAP NF1 (Bloomfield et al., 2015). This mutation allows cells to grow in nutrient-containing media without a bacterial food source (hence axenic). Wild isolates also perform macropinocytosis, although the rate of fluid uptake is too low to allow growth in the standard media used with laboratory-adapted axenic strains. These strains can, however, grow in medium supplemented with additional nutrients (Maeda, 1983; Bloomfield et al., 2015).

Axenic strains form frequent large macropinosomes, which shrink and concentrate their contents once they have been internalised by the cell. The macropinocytic cups are organised around intense patches of active Ras, Rac and plasmanylinositol (3,4,5)-trisphosphate (PIP3) (Hoeller et al., 2013; Parent et al., 1998; Veltman et al., 2016) [note that in *Dictyostelium* PIP3 is a plasmanylinositide, rather than a phosphatidylinositide (Clark et al., 2014)], with SCAR/WAVE and WASP localised to their periphery (Veltman et al., 2016). SCAR/WAVE and WASP activate the Arp2/3 complex to polymerise actin and form the walls of the macropinocytic cup, which is also known as a crown or circular ruffle. The base of the cup appears to be supported by actin polymerisation driven by a Ras-activated formin (Junemann et al., 2016).

The rate of fluid uptake through macropinocytosis by axenic cells is regulated by environmental factors, principally whether the nutrient source for the cells is growth media or bacteria (Kayman and Clarke, 1983; Aguado-Velasco and Bretscher, 1999), and their developmental state (Maeda, 1983; Katoh et al., 2007). Macropinocytosis is additionally affected by the stage of the cell cycle and the concentration of bacterial peptone in the medium (Maeda, 1988), as well as the incubation temperature and the pH (Maeda and Kawamoto, 1986). For certain mutants, fluid uptake is dependent upon whether cells are attached to a surface or in shaking suspension (Novak et al., 1995).

MRC-Laboratory of Molecular Biology, Francis Crick Avenue, Cambridge CB2 0QH, UK.

*Authors for correspondence (rrk@mrc-lmb.cam.ac.uk; thomasw@mrc-lmb.cam.ac.uk)

T.D.W., 0000-0002-0479-5678; R.R.K., 0000-0001-9836-7967

Received 1 December 2017; Accepted 5 February 2018

Journal of Cell Science

Fluid uptake by standard axenic strains of *Dictyostelium*, such as Ax2, is almost entirely due to macropinocytosis (see Discussion) and can be accurately measured by following the uptake of fluorescent dextran as a fluid-phase marker (Kayman and Clarke, 1983; Thilo and Vogel, 1980; Hacker et al., 1997). We have developed a high-throughput assay to measure macropinocytosis in *Dictyostelium*, identified useful inhibitors and sought to better understand how macropinocytosis is physiologically regulated during the switch between macropinocytic and phagocytic feeding and the growth-to-development transition.

RESULTS

Measurement of uptake by high-throughput flow cytometry

Macropinocytosis accounts for more than 90% of fluid uptake by axenic strains of *Dictyostelium*, and can therefore be followed by measuring fluid uptake (Hacker et al., 1997). However, existing methods based on processing individual cell pellets after uptake of fluorescent dextran are relatively low throughput. We therefore developed a high-throughput assay that used flow cytometry to measure TRITC–dextran uptake. The assay is performed in 96-well plates and, after loading with TRITC–dextran, the cells are washed *in situ* by 'dunk-banging' and detached using sodium azide (Glynn and Clarke, 1984) (Fig. 1A), which also prevents exocytosis of internalised dextran (Fig. 1B). Plates are analysed by flow cytometry using a high-throughput sampling attachment to load the flow cytometer, and subsequent analysis is performed with Flowjo, which easily distinguishes *Dictyostelium* cells from beads and bacteria, but not yeast (Fig. 1C). An advantage of flow cytometry is that the fluorescence of internalised TRITC–dextran, a pH-insensitive fluid-phase marker, can be determined for single cells (Fig. 1D). The accumulation of TRITC–dextran proceeds in a uniform fashion across the population over time, with an extended lagging edge of cells with lower uptake. The median fluid internalisation over time by Ax2 cells is quantified in Fig. 1E, while a comparison of uptake rates with previous work (Kayman and Clarke, 1983; Thilo and Vogel, 1980; Aguado-Velasco and Bretscher, 1999; Pintsch et al., 2001; Traynor and Kay, 2007) is shown in Fig. 1F.

Controls show the efficiency of the wash step (Fig. S1A), that the Ax2 cells take up similar volumes of liquid whether in suspension or attached to a surface (as in the assay; Fig. S1B) [although this is not true for all strains (Novak et al., 1995)], and demonstrate the range of cell numbers that can be accommodated per well (Fig. S1C). The assay is calibrated in terms of volume taken up per cell by reference to measurements of uptake by the same cell population undertaken

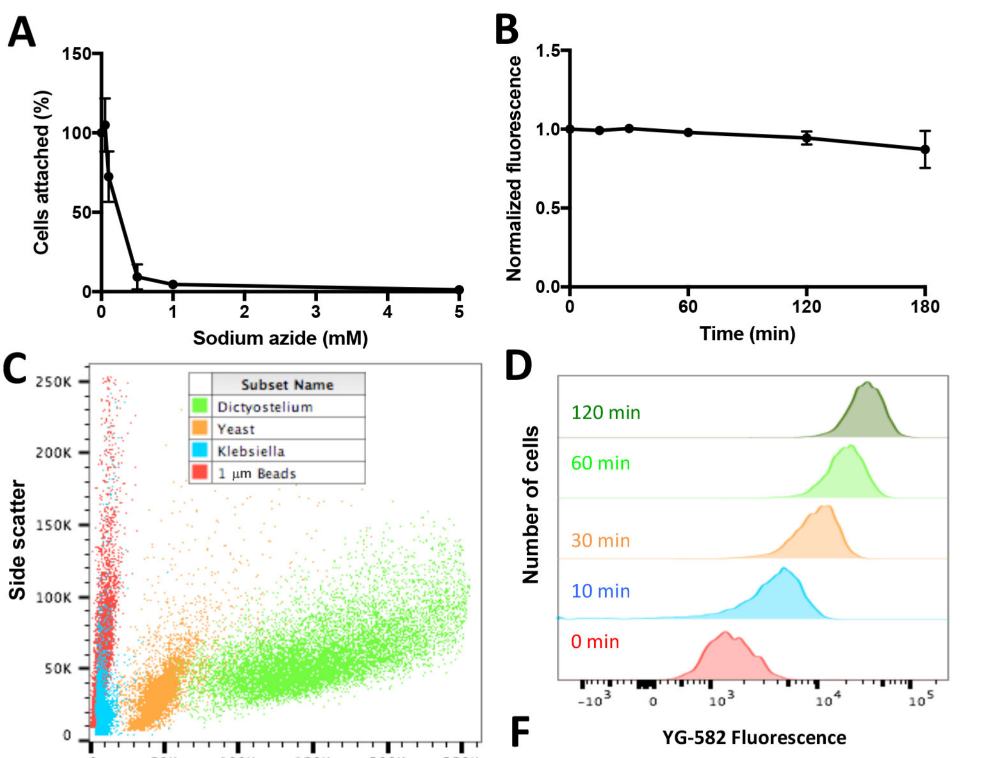

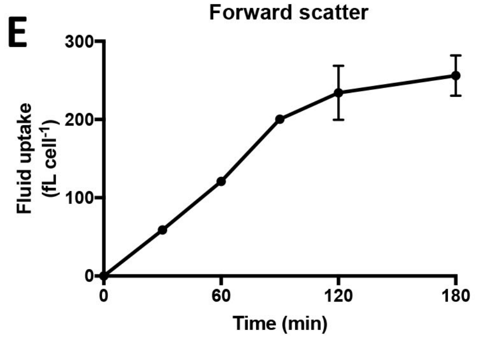

F

Strain	Fluid uptake (fL cell^{-1} h^{-1})	Source
Ax2	120-300	This Work
Ax3	~200	Kayman and Clarke, 1983
Ax2	~250	Aguado-Velasco and Bretscher, 1999
Ax2	~400	Thilo and Vogel, 1980
Ax2	~170	Pintsch et al., 2001
Ax2	~140	Traynor and Kay, 2007

Fig. 1. Fluid uptake measurement by high-throughput flow cytometry. (A) Sodium azide causes efficient detachment of cells in 96-well plates. Attached cells were incubated with sodium azide for 5 min and the proportion remaining attached was measured through Crystal Violet staining (Bloomfield et al., 2015). (B) Sodium azide prevents significant exocytosis of TRITC–dextran for at least 2–3 h. Cells, loaded with dextran, were washed and incubated in 5 mM sodium azide and intracellular fluorescence was measured by flow cytometry. (C) Representative dot-plots showing forward and side scatter for 1 µm beads, bacteria, yeast and *Dictyostelium* cells. *Dictyostelium* are easily distinguished from bacteria, beads and background particles by gating, but cannot be separated fully from yeast particles. (D) Representative histograms showing the internalised TRITC–dextran of individual cells within a population over time. Axenically grown Ax2 cells were incubated in shaking suspension with TRITC–dextran for up to 2 h and analysed by flow cytometry. TRITC–dextran accumulates in every cell, although there is a lagging tail of cells with lower fluid uptake. (E) Fluid uptake timecourse of Ax2 cells in a 96-well plate. TRITC–dextran accumulates linearly for the first 60–90 min, then plateaus as it begins to be exocytosed. (F) A comparison of the fluid uptake by cells in this study with previously published values. All error bars show s.e.m.; *n*=3 in all experiments.

Journal of Cell Science (2018) 131, jcs213736. doi:10.1242/jcs.213736

using a fluorimeter (Fig. S1D) and standardised over time by using Flow-Set fluorosphere calibration beads (Beckman Coulter).

Phagocytosis of beads (Fig. S1E) and bacteria (Fig. S1F), as well as membrane uptake (Fig. S1G), can also be measured in our high-throughput assay. However, as the cells are not shaken, larger beads in particular will settle during the assay, increasing their local concentration and making comparisons between differently sized particles problematic. In addition, all particles tended to make cells detach, limiting the concentration that can be used, and giving uptake rates that are sub-maximal (Sattler et al., 2013). Because of these limitations, particle assays are most suited to making comparisons in standardised conditions, and not for measuring maximal rates. These problems can be circumvented by performing the uptake in shaken suspension, followed by analysis by flow cytometry, but at the cost of throughput.

We standardly use dextran of 155,000 Da for the uptake assays, but since cells may show selectivity in uptake or trafficking of differently sized dextrans, we also tested smaller and larger dextrans (4400 and 500,000 Da), which had similar sensitivity to actin and PIP3 inhibitors (Fig. S1H), consistent with uptake by the same mechanism.

Effect of inhibitors on macropinocytosis

Inhibitors are powerful tools for acutely interfering with biological processes, but relatively few that affect macropinocytosis are currently known. We therefore tested a number of inhibitors affecting both the cytoskeleton and cellular signalling. These were added to Ax2 cells growing in HL5 medium at the start of the uptake assay along with the TRITC–dextran. The internalised fluorescence was measured 1 h later (Table 1). A number of inhibitors were without effect, although whether this was due to lack of inhibitor uptake, target interaction or the target not functioning in macropinocytosis is unknown.

As macropinocytosis is an actin-dependent process, we first tested inhibitors of actin dynamics. Latrunculin B efficiently inhibited macropinocytosis at standard concentrations (Fig. S2A), as expected from its profound effects on the actin cytoskeleton, as did cytochalasin A (Fig. S2B), as previously reported (Hacker et al., 1997). Inhibitors of the Arp2/3 complex (CK666, Fig. S2C), WASP (Wiskostatin, Fig. S2D) and formins (SMIFH2, Fig. S2E) were all potent inhibitors of macropinocytosis, consistent with the localisation of the target proteins to macropinosomes, and genetics showing macropinocytosis defects in WASP^{-} (Veltman et al., 2016) and ForG^{-} (Junemann et al., 2016) mutants and the axenic growth defect of an ArpB mutant (Langridge and Kay, 2007).

The microtubule inhibitors nocodazole (Fig. S2F) and thiabendazole (Fig. S2G) both partially inhibited fluid uptake, indicating a role for microtubules – most likely in macropinosome trafficking (Rai et al., 2016). The myosin II inhibitor blebbistatin had no effect on macropinocytosis up to 100 µM, in contrast to previously published data, which used higher concentrations that precipitated in our conditions (Shu et al., 2005).

Macropinosomes are organised around active Rac, Ras and PIP3-containing patches (Hoeller et al., 2013; Veltman et al., 2016). Accordingly, the phosphoinositide 3-kinase (PI3K) inhibitor LY294002 (Fig. S2H) inhibited fluid uptake, as did TGX221, which targets the mammalian p110β PI3K isoform (Fig. S2I), whereas inhibitors targeting the p110α and p110γ isoforms did not. We found the Rac inhibitor EHT1864 (Shutes et al., 2007) is a potent inhibitor of fluid uptake (Fig. S2J).

Rapamycin, a TORC1 specific inhibitor, did not affect fluid uptake when applied acutely, as found previously, although it does prevent proliferation (Rosel et al., 2012). It has been suggested that mTORC1 has functions that are not inhibited by rapamycin but which can be inhibited by more-potent (but less specific) mTor inhibitors (Thoreen and Sabatini, 2009). We therefore tried

Table 1. Effect of inhibitors on macropinocytosis

Inhibitor	Source	Molecular target(s)	Inhibits macropinocytosis (*P*=<0.05)	IC_{50} (µM)	Maximum inhibition (µM)	Maximum dose tested (µM)
Latrunculin B	Sigma-Aldrich	F-actin	Yes	1	5	10
Cytochalasin A	Cayman	F-actin	Yes	1.7	10	10
Cytochalasin B	Sigma-Aldrich	F-actin	No	N/A	N/A	200
Cytochalasin D	Cayman	F-actin	No	N/A	N/A	200
Jasplakinolide	Santa Cruz	F-actin	No	N/A	N/A	20
CK666	Sigma-Aldrich	Arp2/3	Yes	30	60	100
SMIFH2	Sigma-Aldrich	Formins	Yes	5	30	100
Wiskostatin	Sigma-Aldrich	WASP	Yes	2.75	10	10
Nocodazole	Sigma-Aldrich	Microtubules	Yes	70	70	300
Thiabendazole	Sigma-Aldrich	Microtubules	Yes	70	150	200
Blebbistatin	Sigma-Aldrich	Myosin II	No	N/A	N/A	100
Dynasore	Sigma-Aldrich	Dynamin	No	N/A	N/A	310
LY294002	Cayman	PI3K, TORC2	Yes	38	75	200
BYL719	Cayman	PI3K alpha	No	N/A	N/A	250
TGX221	Cayman	PI3K beta	Yes	60	150	200
CAL101	Cayman	PI3K gamma	No	N/A	N/A	250
EHT1864	Cayman	Rac	Yes	0.03	0.1	0.1
Rapamycin	Sigma-Aldrich	TORC1	No	N/A	N/A	10
PP242	Sigma-Aldrich	TORC1, TORC2	No	N/A	N/A	200
Palomid 529	Sigma-Aldrich	TORC1, TORC2	No	N/A	N/A	500
Torin 1	Sigma-Aldrich	TORC1, TORC2	Yes	20	50	125
Amiloride	Adooq Biosciences	Na^+/H^+ exchanger	No	N/A	N/A	200
EIPA	Cayman	Na^+/H^+ exchanger	No	N/A	N/A	200
EGTA	Sigma-Aldrich	Extracellular Ca^{2+}	No	N/A	N/A	2000

Inhibitors were added at several concentrations to Ax2 cells growing in HL5 medium in 96-well plates in conjunction with TRITC–dextran, and the fluid taken up by the cells in the next hour determined (*n*=3). Dose–response curves are shown for the effective inhibitors ($P<0.05$ using a *t*-test between the maximum tested dose and vehicle-only control) in Fig. S2.

Journal of Cell Science (2018) 131, jcs213736. doi:10.1242/jcs.213736

alternative Tor inhibitors and observed an inhibition of macropinocytosis in cells treated with torin 1 (Fig. S2K), but not palomid 529 or PP242. Whether this is due to greater inhibition of TORC1, inhibition of TORC2, or both is not clear – TORC2 has previously been described as having no function in *Dictyostelium* macropinocytosis (Rosel et al., 2012); however, we see a reduction in macropinocytosis when TORC2 components are knocked out in the Ax2 strain used here (T.D.W., unpublished data).

The nearest to diagnostic inhibitors for macropinocytosis in mammalian cells are amiloride and EIPA, which block the plasma membrane Na^+/H^+ exchanger, thus affecting sub-membranous pH (Koivusalo et al., 2010). Although *Dictyostelium* possesses two Na^+/H^+ exchangers (Patel and Barber, 2005; Fey et al., 2013), it is not known whether they are sensitive to these drugs and we find that the drugs do not affect macropinocytosis. The removal of extracellular Ca^{2+} by means of EGTA inhibits constitutive macropinocytosis in immune cells (Canton et al., 2016), but had no effect on macropinocytosis by *Dictyostelium* incubated in a Ca^{2+}-free medium (50 mM lysine and 55 mM glucose in 50 mM MES pH 6.5) indicating that extracellular Ca^{2+} is not required. Indeed, high extracellular Ca^{2+} concentrations can inhibit *Dictyostelium* macropinocytosis (Maeda and Kawamoto, 1986).

These results support previous genetic studies showing that macropinocytosis depends on PI3K, Rac and actin dynamics controlled through SCAR/WAVE, WASP and formins. On the other hand, regulation through extracellular Ca^{2+} is not part of a conserved core mechanism of macropinocytosis across species, while roles for the Na^+/H^+ exchanger and Tor have not been confirmed for *Dictyostelium* in this work.

Slow switching between feeding strategies

Ax2 cells grown on bacteria have a low rate of macropinocytosis, which increases greatly when they are switched to HL5 growth medium (a complex medium containing peptone, yeast extract and glucose). A similar, although much reduced, increase is seen in wild-type NC4 cells (which have an intact NF1 gene) in media enriched with protein (Maeda, 1983).

We confirmed the upregulation of macropinocytosis in Ax2 cells switched from growth on bacteria to growth on HL5 medium (Fig. 2A). It is slow, taking ∼10 h (Fig. 2B), similar to what is seen for Ax3 cells (Kayman and Clarke, 1983), and involves both an increased rate of macropinosome formation (Fig. 2C) and increased macropinosome size (Fig. 2D). A 50% increase in diameter, as seen here, would lead to an ∼3.4-fold increase in macropinosome volume.

Wild-type DdB cells (the parent of the standard Ax2, Ax3 and Ax4 strains) with an intact NF1 gene only marginally upregulate macropinocytosis in HL5 medium (Fig. 2A). However, if DdB cells are switched to HL5 medium supplemented with 10% fetal calf serum (FCS; Gibco, providing ∼4 mg ml^{-1} additional protein), in which they can proliferate (Bloomfield et al., 2015), they substantially upregulate macropinocytosis, although not as much as Ax2 cells. The increased fluid uptake by DdB cells in this case appears to be due only to an increased rate of macropinosome formation (Fig. 2E), with no detectable increase in size (Fig. 2F). Thus, the macropinocytic rate of wild-type cells is also controlled by the availability of environmental nutrients, as in Ax2 cells.

The ability of *Dictyostelium* cells to ingest large particles, such as yeast, and large volumes of fluid are linked, since both depend on the loss of NF1. Fig. S3A shows the same linkage exists at a physiological level: axenically adapted Ax2 cells (high fluid uptake) phagocytose 2 µm beads better than the same cells grown on bacteria (low fluid uptake). Phagocytosis of smaller 1.75 µm beads is similar between the conditions, while cells grown on bacteria are better at phagocytosis of 1.5 µm beads. Bead uptake by DdB cells, with an intact NF1 gene, is largely unaltered by the nutritional history of the cell (Fig. S3B), consistent with the unaltered macropinosome size of DdB cells observed in Fig. 2F.

Similar trends are apparent when uptake is performed in shaken suspension: axenically adapted Ax2 cells phagocytose yeast better than Ax2 cells grown on bacteria, while DdB is essentially unable to phagocytose yeast in any condition (Fig. S3C). Similarly, axenically adapted Ax2 cells are relatively better at taking up larger 2 µm beads than bacterially grown cells (Fig. S3D).

The macropinocytic and phagocytic states are not mutually exclusive, as we found that Ax2 cells fully adapted to HL5 medium maintain a relatively high rate of phagocytosis of bacteria (Fig. S3E). We therefore asked what happens when Ax2 cells are presented with both bacteria and liquid medium for food. In this case, irrespective of whether the cells had been grown on bacteria or HL5, they adopted a low rate of macropinocytosis (Fig. S3F).

These results show that *Dictyostelium* has two basic feeding modes: the preferred mode is phagocytosis, which is seen with cells growing on bacteria (although these cells retain a low level of macropinocytosis, as noted in Fig. 2C). Cells in nutrient-containing media without bacteria adopt a second mode where macropinocytosis is upregulated, although the potential for phagocytosis of bacteria is retained.

A minimal set of soluble nutrients can stimulate the upregulation of macropinocytosis

Ax2 cells do not sustainably increase their rate of macropinocytosis when they are switched from bacteria to KK_2MC buffer (Fig. 2B), but require HL5 medium, or some components of it, to do so. To identify such stimulatory components, we first showed that HL5 medium could be replaced by the defined medium SIH (Fig. 3A) and then dissected this defined medium to find the active components. Leaving out blocks of components showed that vitamins and micro-minerals are not necessary for macropinocytic upregulation and that the effect is accounted for by amino acids and glucose alone (Fig. 3B). Testing amino acids individually showed that only arginine, lysine and glutamate induce macropinocytosis upregulation at the tested concentrations (Table S1). Consistent with this, removal of just these three amino acids from SIH severely impairs the ability of cells to upregulate macropinocytosis, which is restored when the amino acids are returned to the medium (Fig. 3C). Testing different sugars showed that only glucose and other metabolisable sugars that can support cell growth permit macropinocytosis upregulation (Table S2) (Watts and Ashworth, 1970; Ashworth and Watts, 1970).

Based on these results, a simplified medium for macropinocytosis upregulation, simple upregulation medium (SUM) was devised, consisting of KK_2MC buffer plus 55 mM glucose, 4 mM arginine, 3.7 mM glutamate and 8.5 mM lysine (the same concentrations as SIH) at pH 6.5. SUM induces nearly the same level of macropinocytosis as complete SIH, with faster upregulation kinetics (Fig. 3D). Although cells remain healthy in SUM for several days, it does not support long-term growth. SUM has very low background fluorescence, and we have found it very useful for microscopy, particularly for cells with weakly expressed markers, such as cells with fluorescent tags knocked-in to an endogenous gene. Cells can be grown rapidly on bacteria before transfer to SUM a few hours prior to microscopy, during which time macropinocytosis is greatly upregulated.

These results show that macropinocytosis upregulation can be induced by only a handful of the components present in defined medium, while the requirement for the sugar to be metabolisable

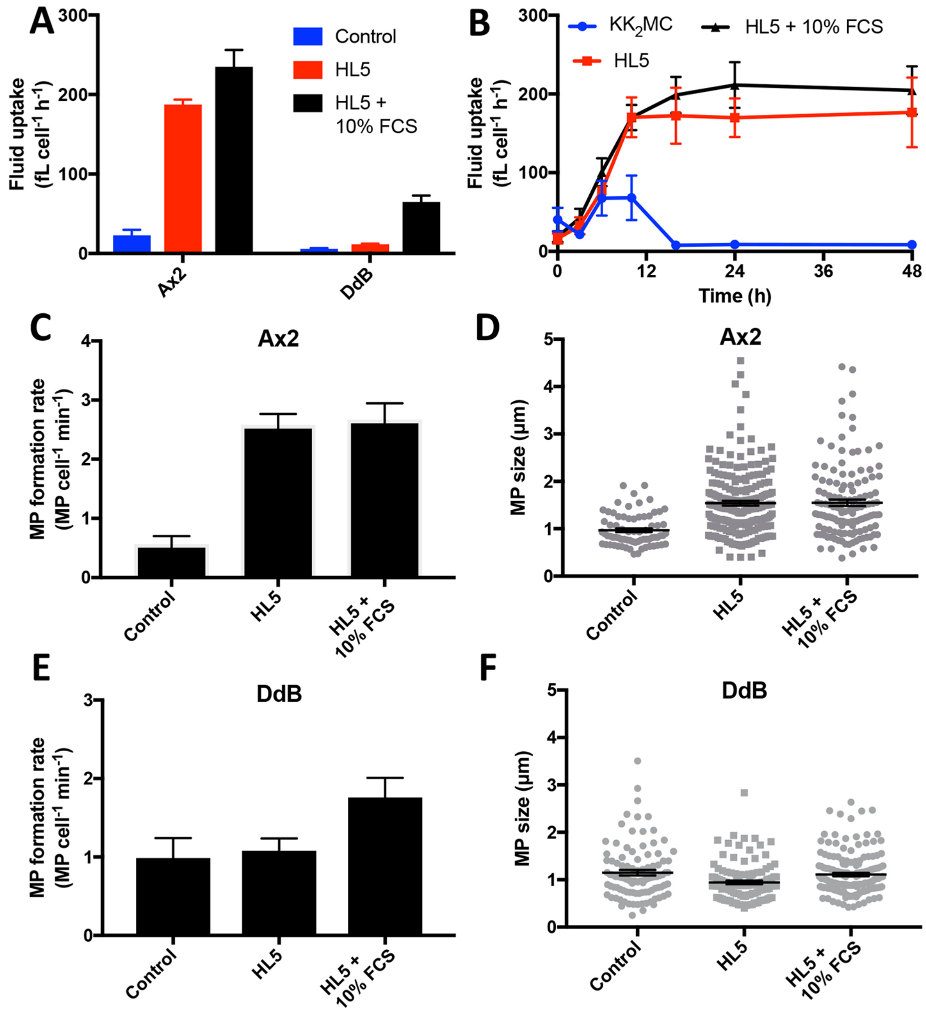

Fig. 2. Cells adapt to growth on liquid media by increasing their rates of fluid uptake and macropinocytosis. (A) Macropinocytosis increases when cells grown on bacteria are transferred to liquid medium. Fluid uptake was either measured immediately after harvesting cells from bacteria (control) or after 24 h in the indicated media (*n*=3). Conditions were compared against the control by unpaired *t*-test and all had $P<0.02$. (B) Kinetics of the increase in fluid uptake by Ax2 cells during adaptation to nutrient-containing media (*n*=3). The cell density is too low for multicellular development to be induced when in KK_2MC buffer. (C) The rate of macropinosome formation increases in Ax2 cells adapted to nutrient-containing media. Macropinosome formation was measured by microscopy of cells fixed after a 1 min pulse with FITC–dextran (*n*=6, $P<0.0001$ for both conditions compared to the control by unpaired *t*-test). (D) The size of macropinosomes increases in Ax2 cells adapted to nutrient-containing media. The maximum diameter of macropinosomes at the moment of closure was measured in the mid-section of cells by using the PIP3 reporter PkgE-PH–mCherry on three separate days ($P<0.0001$ for both conditions compared to the control by unpaired *t*-test). (E) Macropinosome formation increases in DdB cells adapted to HL5 fortified with 10% FCS (*n*=6, $P=0.057$ unpaired *t*-test, compared against the control). (F) Macropinosome size does not increase in DdB cells adapted to liquid media (cells in HL5 had a slight decrease in size compared to the control, whereas cells in HL5+10% FCS showed no difference in size: $P=0.55$ by unpaired *t*-test). Cells were imaged on three separate days. Ax2 is a standard laboratory strain able to grow in HL5 medium due to the absence of an NF1 gene. DdB is its non-axenic parent with an intact NF1 gene. Cells were grown on bacteria, washed and then transferred to the indicated media. Excluding panel B, the control measurements were made with cells freshly harvested from bacteria and the other measurements were made after 24 h incubation in the indicated media. Fluid uptake and other measurements were made as described in the Materials and Methods. Error bars show the s.e.m.

hints that sugars may be sensed through their effects on metabolism, rather than by dedicated receptors.

Macropinocytosis is required for efficient upregulation of macropinocytosis

We envisioned that nutrients that cause macropinocytosis upregulation might either be sensed by dedicated receptors, such as those for glutamate, or indirectly through their effect on metabolism, or a combination of both. Since nutrients obtained by macropinocytosis can only be utilised after internalisation, this second route implies that macropinocytic upregulation would depend on fluid uptake by macropinocytosis itself. To test this idea, we used inhibitors to block macropinocytosis during upregulation. As this experiment requires prolonged inhibitor treatment, we first tested how well cells recover from the inhibitors. Ax2 cells growing in HL5 medium recover quite well from prolonged treatment with LY294002 and TGX221 (both PI3K), CK666 (Arp2/3 complex), EHT1864 (Rac) and torin 1 (Tor) (Fig. S4A–E). Prolonged incubation with other inhibitors was too deleterious to make them useful for these experiments.

We next used the inhibitors to determine to what extent upregulation of macropinocytosis depends on macropinocytosis (Fig. 4, ‘raw’ curves), also making a correction for the relatively small deleterious effects of long-term exposure of cells to the

Journal of Cell Science (2018) 131, jcs213736. doi:10.1242/jcs.213736

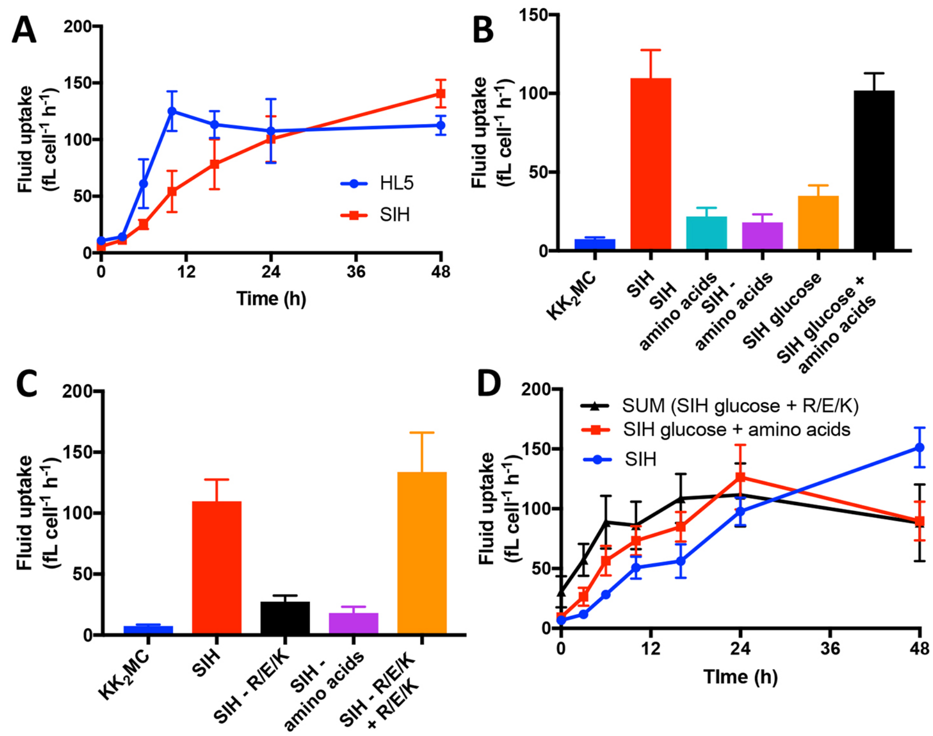

Fig. 3. Macropinocytosis upregulation can be induced by a minimal medium containing glucose, arginine, lysine and glutamate. (A) The defined medium SIH efficiently induces upregulation of macropinocytosis in cells transferred from bacteria. Fluid uptake in the complex HL5 medium is also shown for comparison (n=3). (B) Broad dissection of SIH medium shows that the amino acids and glucose are responsible for its ability to stimulate macropinocytosis upregulation (n=7, P=0.7 by unpaired t-test between SIH and SIH glucose+amino acids). (C) Detailed dissection of SIH medium shows that arginine, glutamate and lysine (R, E and K) are needed for efficient upregulation of macropinocytosis (n=5, P=0.0004 for SIH compared to SIH−R/E/K and 0.5 for SIH compared to SIH−R/E/K+R/E/K by unpaired t-tests). (D) A minimal medium containing only the arginine, glutamate, lysine and glucose in SIH (SUM) gives efficient upregulation of macropinocytosis. The kinetics of upregulation induced by SUM, SIH glucose and amino acids and SIH are compared (n=3). Ax2 cells grown on bacteria were washed free of bacteria and transferred to the indicated media for 24 h, unless indicated otherwise, and then fluid uptake measured by flow cytometry as described in the Materials and Methods. Error bars show the s.e.m.

inhibitors (Fig. 4, ‘corrected’ curves). Although these inhibitors affect macropinocytosis through different targets, they all inhibit upregulation of macropinocytosis (measured after 10 h incubation in HL5 medium) in a dose-dependent manner (Fig. 4A–E). The effect remains even after correcting for the long-term effects of the inhibitors. Upregulation is not completely abolished by the inhibitors, reflecting their incomplete inhibition of macropinocytosis. Thus, these results suggest that the upregulation of macropinocytosis in nutrient-containing media is at least partially dependent on delivery of nutrients into the cell through macropinocytosis.

We considered the possibility that the ingested nutrients delivered by macropinocytosis might be detected through the TORC1 complex, similar to the situation in other organisms. Although rapamycin does not inhibit macropinocytosis acutely, it does somewhat inhibit upregulation (Fig. 4F), with extremely mild effects on control cells (Fig. S4F). Torin 1 has a stronger effect on upregulation (Fig. 4E), but as it is less specific, some of this might be due to inhibition of the TORC2 complex. In summary, these results suggest that nutrients causing cells to increase their rate of macropinocytosis are detected in the macropinocytic pathway, possibly by TORC1.

Sensing of bacteria

Bacteria have two distinct effects on the regulation of macropinocytosis. They inhibit upregulation of macropinocytosis in cells that are transferred into HL5 medium after being previously grown on bacteria (Fig. 5A), and promote downregulation of macropinocytosis by cells transferred from HL5 medium to KK_2MC buffer where it otherwise would remain high (Fig. 5B, see later).

Bacteria can be sensed through their release of folate, which is a chemoattractant for *Dictyostelium* and acts through the G-protein-coupled receptor fAR1 (Pan et al., 2016). We found that folate inhibits the upregulation of macropinocytosis when cells are transferred from bacteria to HL5 medium (Fig. 5C), but has no effect when cells are transferred from HL5 medium to KK_2MC buffer (data not shown). fAR1-null cells are essentially blind to this inhibitory effect of folate (Fig. 5D), as are mutants of the Gβ and Gα4 (Hadwiger and Firtel, 1992), subunits of the cognate heterotrimeric G-protein for fAR1 (Fig. 5E) (Hadwiger and Srinivasan, 1999), and ErkB (Fig. 5F), the downstream MAP kinase. Thus, bacteria can exert some, but clearly not all, of their effects on feeding behaviour through canonical folate signalling.

Developmental regulation of macropinocytosis

Development in *Dictyostelium* is triggered by starvation and, over the first 8–10 h, the cells undertake chemotaxis towards cyclic AMP causing them to aggregate. Macropinocytosis is downregulated during this period (Maeda, 1983; Katoh et al., 2007), and it was therefore surprising that macropinocytosis continues at a high rate for at least 24 h in cells starved by incubation in KK_2MC buffer (Fig. 5B). However, compared to standard developmental conditions, these cells were starved at low density, likely causing attenuation of developmental signalling. This suggests that the

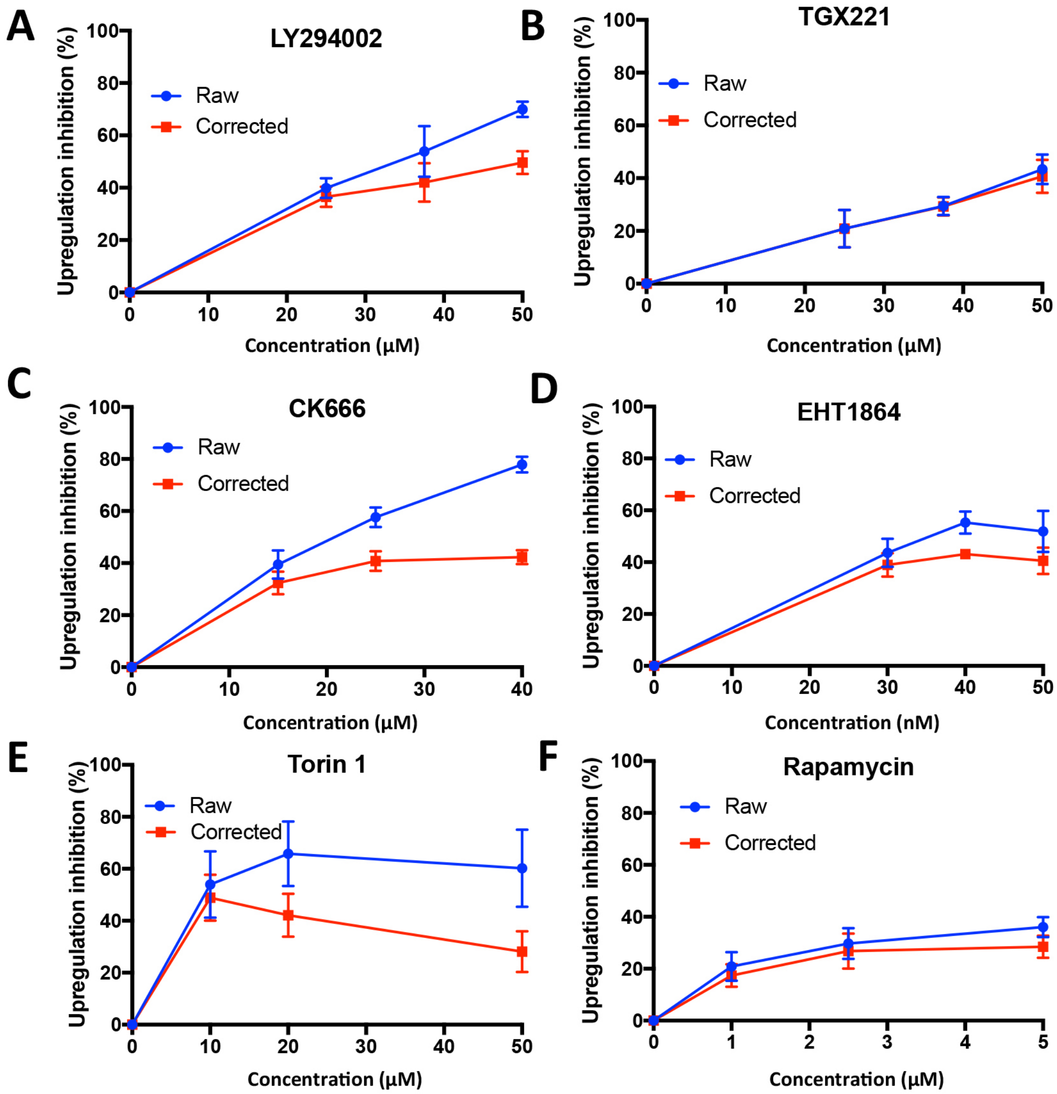

Fig. 4. Evidence that macropinocytosis upregulation depends on macropinocytosis. To test whether macropinocytosis upregulation depends on macropinocytosis, inhibitors with differing targets (see Table 1) were used to inhibit macropinocytosis during the upregulation period. The inhibitor was then washed away and the degree of upregulation determined by measuring fluid uptake compared to untreated controls ('raw' curves). To control for long-term effects of the inhibitors, cells with fully upregulated macropinocytosis were treated in parallel and the results corrected accordingly ('corrected' curves; see Fig. S4). Inhibitors used and their nominal targets were: (A) LY29004 (PI3K, *n*=3); (B) TGX221 (PI3K, *n*=4); (C) CK666 (Arp2/3 complex, *n*=4); (D) EHT1864 (Rac, *n*=4); (E) Torin 1 (Tor, *n*=3); and (F) rapamycin (TORC1, *n*=3). Ax2 cells, harvested from bacteria, were incubated in HL5 in 96-well plates with the inhibitors for 10 h, then the inhibitors were washed away by dunk-banging and the cells allowed to recover for 10 min before the fluid uptake was measured over 1 h using the high-throughput flow cytometry assay. To correct for deleterious effects of the inhibitors, control Ax2 cells grown in HL5 (with maximally upregulated macropinocytosis) were similarly treated with inhibitors for 10 h and their fluid uptake compared to untreated controls to give the correction factor as Uptake (drug-treated control cells)/Uptake (vehicle-treated control cells), by which the raw data was multiplied to give the corrected curves. Error bars show the s.e.m.

downregulation of macropinocytosis during development requires a developmental signal in addition to starvation.

Fig. 6A confirms that macropinocytosis is strongly downregulated by starving Ax2 cells (previously grown in HL5) at high density in shaking suspension and pulsed with cyclic AMP to mimic developmental signalling. By 5 h of development, fluid uptake is negligible. Similar results were obtained when developing cells on non-nutrient agar (Fig. S5A). Similarly, if the cell density in 96-well plates is increased from 5000 to 50,000 cells per well, the cells form visible aggregates and also downregulate their macropinocytosis (Fig. 6B).

Later in development, tight aggregates form, which could distort uptake assays by restricting access of dextran to internal cells. However, the main decline in macropinocytosis occurs before this stage (Fig. S5B,C) and we see no evidence for two populations of cells (inner and outer) in the flow cytometry results, suggesting that restricted access to internal cells does not significantly affect our results, at least in the first 6 h of development.

We tested the effects of known developmental signals on macropinocytosis using cells starving at low cell density. As shown in Table S3, the developmental signals cyclic AMP, ATP (Ludlow et al., 2008; Traynor and Kay, 2017), adenosine and the polyketides DIF-1, DIF-2 and MPBD (Morris et al., 1987, 1988; Saito et al., 2006) were without effect, as was the high-cell density signal polyphosphate (Suess and Gomer, 2016). However, conditioned medium (CM) prepared by shaking starving cells at high density for 8 h was effective at inhibiting macropinocytosis, with the active component(s) being heat-labile and retained by a

Journal of Cell Science (2018) 131, jcs213736. doi:10.1242/jcs.213736

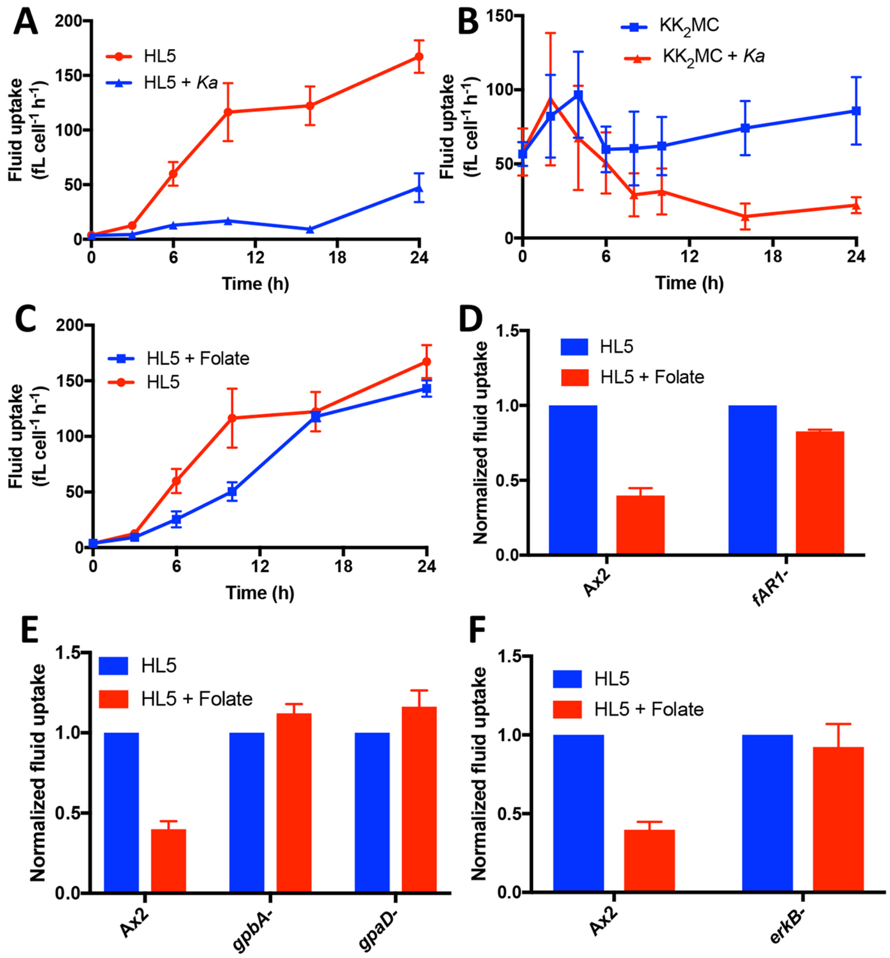

Fig. 5. Long-term regulation of macropinocytosis by bacteria and their product, folate. (A) Bacteria inhibit the upregulation of macropinocytosis in cells transferred to HL5 medium. Ax2 cells transferred from bacteria (low macropinocytosis) to HL5 upregulate macropinocytosis, but this is blocked by addition of *Ka* bacteria (2 $OD_{600\ nm}$) to the HL5 (*n*=6). (B) Bacteria induce downregulation of macropinocytosis by cells taken from HL5 medium. Ax2 cells transferred from HL5 medium (high macropinocytosis) to KK_2MC buffer maintain their rate of macropinocytosis (the cell density is too low for development), but the addition of 2 $OD_{600\ nm}$ *Ka* bacteria induces downregulation (*n*=6). (C) Folate delays the upregulation of macropinocytosis in cells transferred to HL5 medium. Ax2 cells transferred from bacteria (low macropinocytosis) to HL5 medium upregulate macropinocytosis, but this is delayed upon addition of 500 µM folate (*n*=6, *P*=0.025 by unpaired *t*-test at 6 h upregulation). (D) The folate receptor (fAR1) mediates the inhibitory effect of folate on macropinocytosis upregulation. Wild-type Ax2 cells and a null mutant for the folate receptor (*fAR1*$^-$) were transferred from bacteria (low macropinocytosis) to HL5 medium with or without 500 µM folate and macropinocytosis measured after 6 h (*n*=5, comparing the values of the folate treated cells, *P*=0.0004 by unpaired *t*-test). (E) The heterotrimeric G-protein cognate to the folate receptor mediates the inhibitory effect of folate on macropinocytosis upregulation. Wild-type Ax2 cells and null mutants for Gα4 (*gpaD*$^-$) and Gβ (*gpbA*$^-$) were transferred from bacteria (low macropinocytosis) to HL5 medium with or without 500 µM folate and macropinocytosis was measured after 6 h (*n*=5, comparing the values of the folate treated cells to the untreated cells, *P*=0.18 and 0.07 by unpaired *t*-test for Gα4$^-$ and Gβ$^-$, respectively). (F) The MAP-kinase ErkB, a downstream effector of the folate receptor mediates the inhibitory effect of folate on macropinocytosis upregulation. Wild-type Ax2 cells and null mutants for ErkB (*erkB*$^-$) were transferred from bacteria (low macropinocytosis) to HL5 medium with or without 500 µM folate, and macropinocytosis was measured after 6 h (*n*=3, comparing the values of the folate-treated cells to the untreated cells, *P*=0.65 by unpaired *t*-test). Fluid uptake was measured with the high-throughput flow cytometry. Error bars are the s.e.m.

30 kDa cut-off membrane and, therefore, likely to be protein(s) (Fig. 6C). Most likely this signal is one of the known proteins controlling early developmental events in *Dictyostelium*, but unfortunately these were unavailable for testing.

To gain insight into how developmental signals suppress macropinocytosis, we examined possible signal transduction routes, focussing on cyclic AMP-dependent protein kinase (PKA), which is a crucial mediator of both early and late events in development (Mann and Firtel, 1991; Harwood et al., 1992; Kay, 1989). PKA can be directly activated by using the membrane-permeable analogue of cyclic-AMP, 8-bromo-cyclic-AMP (8-Br-cAMP), and we found that this, unlike cyclic AMP, causes up to a 50% downregulation of macropinocytosis in starving cells at low density (Fig. 6D). High concentrations are required, but these are comparable to those used previously (Kay, 1989).

The involvement of PKA is strongly supported by mutants with elevated intracellular cyclic AMP levels, due to defective breakdown. The hybrid cyclic AMP phosphodiesterase RegA is activated by a His/Asp phospho-relay in which RdeA is the essential phosphate carrier protein (Shaulsky et al., 1998; Thomason et al., 1999, 1998; Chang et al., 1998). Elimination of either protein results in strong downregulation of macropinocytosis in starving cells at low density (Fig. 6E).

Conversely, eliminating PKA activity by mutation of the catalytic subunit (*pkaC*$^-$ cells; Primpke et al., 2000) results in cells where macropinocytosis remains high for at least 24 h after starvation,

Journal of Cell Science

Journal of Cell Science (2018) 131, jcs213736. doi:10.1242/jcs.213736

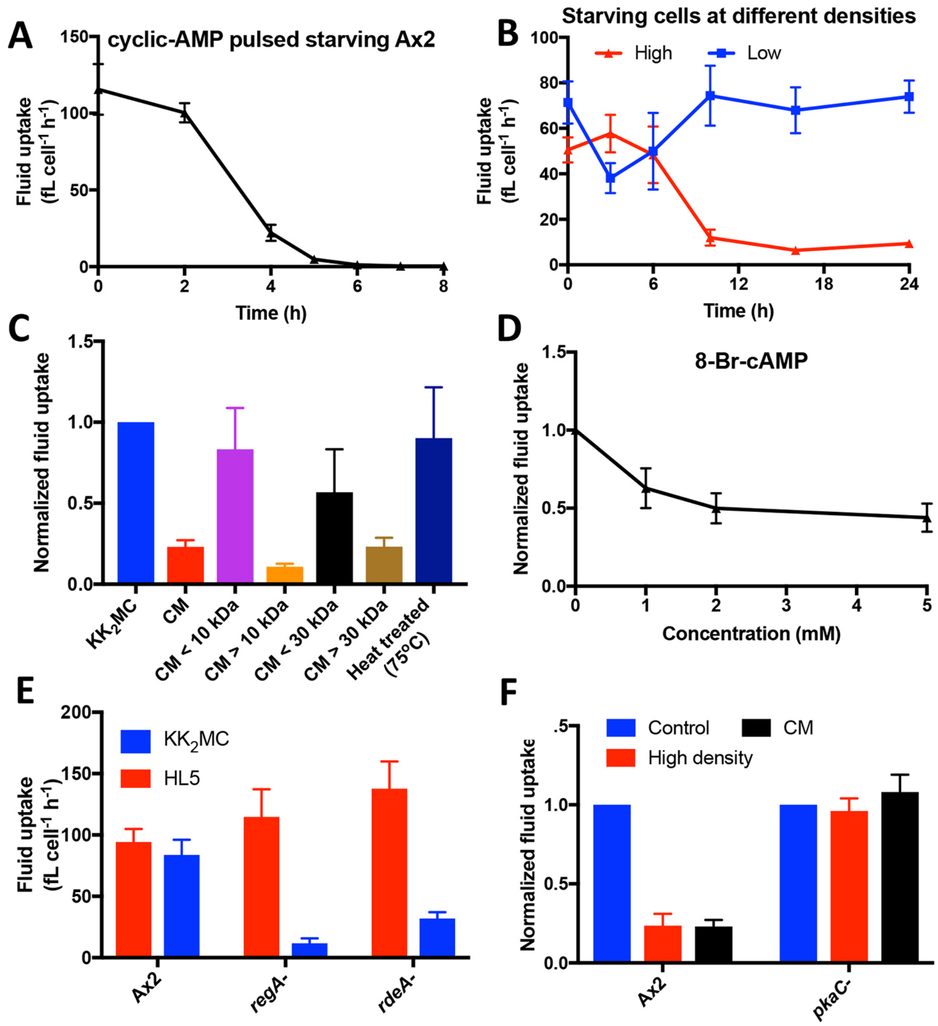

Fig. 6. Macropinocytosis is downregulated by developmental signalling that likely acts through PKA. (A) Macropinocytosis is downregulated during development. Ax2 cells grown in HL5 (high macropinocytosis) were washed free of nutrients and allowed to develop in standard conditions: shaken in suspension and pulsed with cyclic AMP every 6 min after the first hour (*n*=5). (B) Downregulation of macropinocytosis depends on the cell density. Axenically growing cells were allowed to settle at high (50,000 cells well^{-1}) and low (5000 cells well^{-1}) density in 96-well plates, washed free of nutrient media and incubated in KK_2MC buffer for the indicated times before fluid uptake was determined as described in the Materials and Methods (*n*=6). (C) Downregulation of cells at low density is induced by conditioned medium. Conditioned KK_2MC buffer (CM) prepared by shaking starving cells at high density for 8 h was tested for its ability to induce downregulation of macropinocytosis in Ax2 cells. The CM was size-fractionated or heat-treated at 75°C for 30 min to further define the properties of the secreted product responsible for downregulation (*n*=3, *P*<0.0001 for CM and CM >30 kDa compared to KK_2MC buffer by unpaired *t*-test, and 0.77 for heat-treated CM). (D) Downregulation of macropinocytosis in cells at low density incubated for 24 h with 8-Br-cAMP (which activates PKA) (*n*=5). (E) Mutations giving elevated intracellular cyclic AMP levels bypass the need for developmental signalling to downregulate macropinocytosis. *regA*$^-$ and *rdeA*$^-$ cells have elevated intracellular cyclic AMP due to reduced breakdown, and downregulate macropinocytosis when incubated in KK_2MC buffer for 24 h, unlike Ax2 (*n*=5, for unpaired *t*-tests between HL5 and KK_2MC buffer *P*=0.0003 for *rdeA*$^-$ and *regA*$^-$ and 0.53 for Ax2). (F) Macropinocytosis is not downregulated in a mutant lacking PKA activity (*pkaC*$^-$), even when incubated in CM or at high density in KK_2MC buffer (*n*=6). Error bars show the s.e.m.

even when they are at high cell density or treated with CM (Fig. 6F). Combined, these results strongly argue that macropinocytosis is downregulated in starving cells because of PKA activation. These results are also relevant to the interpretation of recent work (Scavello et al., 2017) showing that *pkaC*− cells have a strong defect in chemotaxis towards cyclic AMP (see Discussion).

DISCUSSION

The great majority of fluid uptake by axenic *Dictyostelium* cells is by macropinocytosis, rather than, for instance, by clathrin-mediated endocytosis. This has been shown through morphometry (Hacker et al., 1997), the sensitivity of fluid uptake to mutations and inhibitors specifically expected to affect macropinocytosis, such as those affecting PI3K and the RasGAP NF1 (Buczynski et al., 1997; Hoeller et al., 2013; Bloomfield et al., 2015; Veltman et al., 2016; this work), and finally by the lack of correlation between the uptake of membrane (taken up mainly by clathrin-mediated endocytosis) and fluid in various situations, indicating that they are largely separate processes (Aguado-Velasco and Bretscher, 1999). In this context, the reduced fluid uptake seen in clathrin heavy chain mutants is likely an indirect effect, perhaps due to perturbed processing of macropinosomes (O'Halloran and Anderson, 1992). The various lines of evidence suggest that macropinocytosis accounts for more than 90% of fluid uptake by axenic cells fully adapted to growth on liquid medium.

This high rate of macropinocytosis allows fluid uptake to be used as a measure of macropinocytosis, which is an enormous advantage

Journal of Cell Science

Journal of Cell Science (2018) 131, jcs213736. doi:10.1242/jcs.213736

over assays based on counting macropinosomes visualised by microscopy (Commisso et al., 2014). We have adapted the previous macropinocytosis assays based on bulk fluid uptake (Kayman and Clarke, 1983; Thilo and Vogel, 1980; Rivero and Maniak, 2006) to flow cytometry and 96-well plates, thus giving high-throughput and single-cell resolution.

A screen of inhibitors provides new tools for acute inhibition of macropinocytosis and further supports the involvement of PI3K, Rac, WASP, formins and the Arp2/3 complex, as expected from genetic and subcellular localisation studies (Buczynski et al., 1997; Hoeller et al., 2013; Langridge and Kay, 2007; Dumontier et al., 2000; Veltman et al., 2016; Junemann et al., 2016).

Macropinocytosis in *Dictyostelium* occurs at a high rate in conditions where the cells can proliferate in liquid medium. However, it is under physiological control, with cells slowly transitioning between high and low macropinocytic states according to whether bacteria or soluble nutrients are available. In these transitions, the frequency of macropinosome formation is altered: in axenic cells, where the active Ras patches are unconstrained by NF1, macropinosome size is additionally increased. Wild-type cells with an intact NF1 gene also transition between low and high macropinocytic states according to the nutrients available, showing that this regulation is not just a feature of axenic strains (this work; Maeda, 1983). The presence of a high macropinocytic state in wild-type cells suggests there are ecological circumstances where macropinocytosis is used for feeding, though these are yet to be defined.

Ax2 cells in the low macropinocytic state can sense bacteria through their secretion of folic acid, inhibiting macropinocytic upregulation accordingly. However, due to the relatively modest effects of folate, and the fact that it does not induce downregulation of macropinocytosis, it seems certain that other sensory pathways also play a prominent role. It has recently been reported that certain bacteria secrete cyclic AMP, which functions as a chemoattractant for vegetative *Dictyostelium* (Meena and Kimmel, 2017); however, cyclic AMP did not affect the upregulation or downregulation of macropinocytosis.

Four nutrients are largely responsible for inducing macropinocytosis upregulation in Ax2 cells: arginine, glutamate, lysine and a metabolisable sugar. None of the other amino acids appears effective individually, and even in combination they have only a modest effect. Arginine and lysine are essential amino acids, but glutamate is not (Marin, 1976; Franke and Kessin, 1977). *Dictyostelium* has several receptors similar to metabotropic glutamate receptors (Taniura et al., 2006; Fey et al., 2013), but it seems likely that the major route for nutrient sensing is intracellular, with nutrients delivered by macropinocytosis.

In mammalian cells, free amino acids obtained by macropinocytosis are sensed by activation of mTORC1 at the lysosome (Yoshida et al., 2015; Sancak et al., 2010), with one effect being inhibition of autophagy. In *Dictyostelium*, autophagy is induced within minutes of withdrawing arginine and lysine (King et al., 2011), a step which is necessary to survive prolonged amino acid starvation (Tekinay et al., 2006). Taken together, what is known about mTORC1 and *Dictyostelium* autophagy alongside our results suggests that *Dictyostelium* TORC1 may sense arginine and lysine to upregulate macropinocytosis. Our attempts to test this idea using Tor inhibitors are not definitive, but it remains an attractive possibility.

As only metabolisable sugars induce upregulation of macropinocytosis, it is probable that the sensing of these is through a general metabolic readout, such as the ratio of ATP to ADP and AMP. Increased levels of AMP and ADP, as occurs in nutrient-poor conditions (such as without sugar), activate AMP-kinase. Overexpression of a constitutively active AMP-kinase α subunit in *Dictyostelium* inhibits growth but does not affect macropinocytosis (Bokko et al., 2007), similar to what we observe in low-density starvation conditions. Although an attractive possibility, it remains to be determined whether AMP-kinase has any function in upregulation of macropinocytosis.

Our results show that the cessation of macropinocytosis during early development requires a developmental signal that most likely acts through PKA. Macropinocytosis does not cease immediately when cells are starved, but decreases over several hours and so may occur at reduced levels in cells used for studying chemotaxis to cyclic AMP. This can be a confounding influence since macropinocytosis uses the same actin machinery as pseudopods and thus impairs chemotaxis (Veltman, 2015). In particular, we found that macropinocytosis continues at a high rate in mutants of the PKA catalytic subunit, possibly accounting for the strong chemotactic defect of these strains (Scavello et al., 2017). Continued macropinocytosis could also confound studies on other strains with early developmental defects (Khosla et al., 2005; Wu et al., 1995; Rodriguez et al., 2008; Lee et al., 2005).

Many of the molecular components required for macropinocytosis are the same in both *Dictyostelium* and mammalian cells, such as actin, Arp2/3, PI3K, SCAR/WAVE, WASP, Rac and Ras proteins. This suggests that macropinocytosis may have first arisen in simple protists as a way of feeding in the absence of bacterial prey. In mammalian cells, there are additional levels of regulation, some of which are cell type specific (such as the Ca^{2+} requirement in immune cells) and others that are more generic (such as growth factor-stimulated macropinocytosis). *Dictyostelium* with its high intrinsic rate of macropinocytosis in axenic strains, high-throughput assays (this work), and the recent development of transformation techniques that allow easy manipulation of non-axenic strains – and thus of mutants defective in macropinocytosis (P. Paschke, D. A. Knecht, A. Silale, D. Traynor, T.D.W., P. A. Thomason, R. H. Insall, J. R. Chubb, R.R.K., D. M. Veltman; unpublished data) – is now an excellent model for establishing the conserved core elements of macropinocytosis.

MATERIALS AND METHODS

Cell culture and materials

Cells were cultivated at 22°C. HL5, SIH (complete, and lacking components) and SM media were from Formedium. Unless otherwise specified, cells were grown on *Klebsiella aerogenes* (*Ka*) lawns on SM plates and harvested for experiments from the feeding front, washing three times with KK_2 (16.6 mM KH_2PO_4, 3.8 mM K_2HPO_4, pH 6.1) by centrifugation (280 ***g***, 3 min) to remove the bacteria. Cells were also grown in tissue culture plates with *Ka* as a food source. In this case, *Ka* was added to KK_2MC buffer (KK_2 plus 2 mM $MgSO_4$, 100 µM $CaCl_2$) to 2 optical density units at 600 nm (2 OD_{600nm}) units from a 100 OD_{600nm} stock (the stock bacteria were grown overnight in 2× TY, pelleted by centrifugation, washed twice in KK_2 and stored at 4°C).

Cells were grown axenically in HL5 in conical flasks with shaking at 180 rpm. Media derived from SIH, including SUM, were made in KK_2MC pH 6.5. Conditioned medium was made by washing axenically grown Ax2 cells free of HL5, resuspending them to 10^7 cells ml^{-1} in KK_2MC and incubating for 8 h, with 180 rpm shaking, before removing the cells by centrifugation (2400 ***g***, 10 min). Strains are listed in Table S4.

For transformation, cells were harvested from bacteria, resuspended in H40 buffer (40 mM Hepes, 1 mM $MgCl_2$, pH 7.0), mixed with 500 ng vector for a PIP3 reporter (PkgE-PH–mCherry), electroporated in ice-cold 2 mm cuvettes (Novagen) using a square wave protocol (2×350 volts, 8 ms apart), and then transferred to 2 ml KK_2MC+*Ka* in a six-well plate to recover for 5 h, before G418 selection was added to 10 µg ml^{-1} (Paschke et al., in revision).

Journal of Cell Science

Chemicals were from Sigma unless otherwise indicated. Polyphosphate was from both Spectrum and Merck.

Uptake measurements by fluorimetry

The method used was based on that from Rivero and Maniak, 2006. Cells at 1×10^7 ml^{-1} were shaken at 180 rpm in HL5 with 0.5 mg ml^{-1} TRITC–dextran (molecular mass of 155,000 Da, unless otherwise stated) and at each time point triplicate 0.8 ml samples were centrifugally washed once in ice-cold KK_2 and resuspended to 1 ml. Fluorescence was measured in a fluorimeter (Perkin-Elmer LS 50 B with excitation at 544 nm, emission at 574 nm, slit width 10 nm). Background '0 minute' fluorescence was subtracted and uptake volume was calculated from standard curves for TRITC–dextran diluted in buffer. Cells loaded in this way were also analysed by flow cytometry (LSR_II flow cytometer, BD Biosciences) to compare the methods.

To measure yeast uptake, cells were resuspended to 5×10^6 cells ml^{-1} in KK_2MC in a 5 ml conical flask and shaken at 180 rpm at 22°C. TRITC-labelled yeast (sonicated at level 7.0 for 20 s on a Misonix sonicator 3000) were added to 10^7 particles ml^{-1}. At 0 and 60 min, duplicate 200 µl samples were added to 20 µl of Trypan Blue quench solution (2 mg ml^{-1} in 20 mM citrate, 150 mM NaCl, pH 4.5) on ice, shaken for 3 min at 2000 rpm, spun down and washed twice with ice-cold KK_2+10 mM EDTA. The final pellet was resuspended to 1 ml and the fluorescence compared to a standard curve to give the number of yeast per cell.

Uptake measurements by flow cytometry

For high-throughput assays, 50 µl of medium with 10^5 cells ml^{-1} was incubated in flat-bottom, 96-well plates at 22°C for the indicated time (usually 24 h). Then 50 µl of 1 mg ml^{-1} TRITC–dextran in the same medium was added for a final concentration of 0.5 mg ml^{-1}. After 1 h, unless otherwise stated, the medium was thrown off, and the cells washed by 'dunk-banging' (the plate was submerged in a container of ice-cold KK_2, which was thrown off and the plate patted dry) before 100 µl KK_2MC containing 5 mM sodium azide was added to each well to detach the cells and stop exocytosis. Cells were analysed by flow cytometry (LSR-II, BD Biosciences) using the high-throughput sampling attachment, which pipetted them up and down twice, before analysing 65 µl per sample at 3 µl s^{-1}. FlowJo software (https://www.flowjo.com) calculated the median fluorescence of cells in each well. The mean was then taken of all biological replicates. To determine volumes taken up, the same population of cells (loaded with TRITC–dextran in suspension, as above) was analysed by both fluorimetry and flow cytometry. The LSR-II flow cytometer was calibrated through all subsequent experiments by using FlowSet fluorospheres calibration beads (Beckman Coulter).

We also used this method to measure uptake of membrane using 10 µM FM1-43 (Invitrogen), phagocytosis of bacteria using 1×10^8 particles ml^{-1} Texas Red *E. coli* bioparticles (Thermo Scientific), or beads of different sizes (YG-beads, Polysciences; 2.0 and 1.75 µm at 5×10^7 ml^{-1}, 1.0 and 1.5 µm at 10^8 ml^{-1}). Bead uptake in shaking suspension was measured by using cells at 2×10^6 cells ml^{-1} in KK_2MC (prepared as for the yeast uptake assay) with 4×10^8 beads ml^{-1}. After shaking at 180 rpm for 20 min, samples were diluted into ice-cold KK_2+5 mM NaN_3, spun down (300 ***g***, 3 min), washed once, then resuspended and filtered into tubes for flow cytometry. The number of particles internalised per cell were calculated as described (Sattler et al., 2013). Beads larger than 2 µm were taken up very poorly, so were not used. For time courses, start times were staggered so that all incubations ended concurrently. When inhibitors were used acutely, they were added with the fluorescent medium to the final indicated concentration. Polyketides were synthesised as described (Morris et al., 1987, 1988; Saito et al., 2006).

To initiate development, axenically growing cells were washed twice, resuspended to 10^7 cells ml^{-1} in KK_2MC and shaken at 180 rpm for 1 h before delivering pulses of KK_2MC containing cyclic AMP to give a concentration of 100 nM every 6 min using a Watson Marlow 505Di pump. At the indicated times 5×10^4 cells were diluted into dextran-containing KK_2MC in 24-well plates for 1 h, after which they were washed *in situ* using ice-cold KK_2+10 mM EDTA and detached with KK_2MC+5 mM sodium azide. 100 µl was transferred to duplicate wells in a 96-well plate for flow cytometry analysis.

Development on non-nutrient agar plates was initiated by settling 1.5 ml of washed, axenically growing cells at 2.5×10^7 cells ml^{-1} in KK_2MC onto fresh 1.8% KK_2MC agar (Oxoid L28) in 6-cm plates. After 15 min settling, the medium was aspirated off, and the plates kept on wet tissues at 22°C. At the indicated times, cells were harvested, resuspended in KK_2MC and 10^5 cells inoculated into KK_2MC in a six-well plate with 0.5 mg ml^{-1} TRITC-dextran for 1 h. Cells were then washed *in situ* and resuspended in KK_2+10 mM EDTA before analysis by low-throughput flow cytometry. The zero hour time point was for cells taken immediately after washing.

Macropinosome formation rate and diameter

The rate of macropinosome formation was determined in KK_2MC by loading cells in a two-well microscope slide (Nunc) with 2 mg ml^{-1} FITC–dextran (molecular mass 70,000 Da) for 1 min, then washing and fixing with 4% paraformaldehyde for 20 min. Fixed cells were washed five times and stored in PBS (pH 5.0) at 4°C for imaging. *Z*-stacks with 0.1 µm steps were taken using a Zeiss 700 series microscope with 2× averaging to reduce noise. Maximum intensity projections were made using FIJI and FITC-positive endosomes counted by eye. The mean of at least eight cells on a given day was taken as one data point.

To measure macropinosome diameter at closure, cells in KK_2MC expressing a PIP3 reporter (PkgE-PH–mCherry) were filmed in their central section at 1 frame per second for 5 min on a Zeiss 700 series microscope. The maximum diameter of macropinosomes at closure was measured by using the FIJI measure tool. Note that this method will underestimate the diameter of macropinosomes not lying fully within the optical section.

Acknowledgements
We thank the rest of the Kay laboratory for their assistance in moulding this project, particularly Peggy Paschke. Clelia Amato and Robert Insall (Beatson Institute, Glasgow) alerted us to the Rac inhibitor. Jason King (Sheffield University) provided valuable feedback on the macropinosome formation experiments. Miao Pan and Tian Jin (NIAID, Bethesda) kindly sent us the *fAR1*$^-$ strain. The MRC-LMB flow cytometry facility maintained the flow cytometers and provided technical support.

Competing interests
The authors declare no competing or financial interests.

Author contributions
Conceptualization: T.W., R.R.K.; Methodology: T.W.; Validation: T.W.; Investigation: T.W.; Resources: R.R.K.; Writing - original draft: T.W.; Writing - review & editing: T.W., R.R.K.; Visualization: T.W.; Supervision: R.R.K.; Project administration: R.R.K.; Funding acquisition: R.R.K.

Funding
We thank the Medical Research Council UK for core funding (U105115237) to R.K. Deposited in PMC for release after 6 months.

Supplementary information
Supplementary information available online at
http://jcs.biologists.org/lookup/doi/10.1242/jcs.213736.supplemental

References
Aguado-Velasco, C. and Bretscher, M. S. (1999). Circulation of the plasma membrane in *Dictyostelium*. *Mol. Biol. Cell* **10**, 4419-4427.

Ashworth, J. M. and Watts, D. J. (1970). Metabolism of the cellular slime mould *Dictyostelium discoideum* grown in axenic culture. *Biochem. J.* **119**, 175-182.

Bacon, R. A., Cohen, C. J., Lewin, D. A. and Mellman, I. (1994). *Dictyostelium discoideum* mutants with temperature-sensitive defects in endocytosis. *J. Cell Biol.* **127**, 387-399.

Bloomfield, G. and Kay, R. R. (2016). Uses and abuses of macropinocytosis. *J. Cell Sci.* **129**, 2697-2705.

Bloomfield, G., Traynor, D., Sander, S. P., Veltman, D. M., Pachebat, J. A. and Kay, R. R. (2015). Neurofibromin controls macropinocytosis and phagocytosis in *Dictyostelium*. *eLife* **4**, e04940.

Bokko, P. B., Francione, L., Bandala-Sanchez, E., Ahmed, A. U., Annesley, S. J., Huang, X., Khurana, T., Kimmel, A. R. and Fisher, P. R. (2007). Diverse cytopathologies in mitochondrial disease are caused by amp-activated protein kinase signaling. *Mol. Biol. Cell* **18**, 1874-1886.

Buckley, C. M. and King, J. S. (2017). Drinking problems: mechanisms of macropinosome formation and maturation. *FEBS J.* **284**, 3778-3790.

Buczynski, G., Grove, B., Nomura, A., Kleve, M., Bush, J., Firtel, R. A. and Cardelli, J. (1997). Inactivation of two Dictyostelium discoideum genes, DdPIK1 and DdPIK2, encoding proteins related to mammalian phosphatidylinositide

3-kinases, results in defects in endocytosis, lysosome to postlysosome transport, and actin cytoskeleton organization. *J. Cell Biol.* **136**, 1271-1286.

Canton, J., Schlam, D., Breuer, C., Gütschow, M., Glogauer, M. and Grinstein, S. (2016). Calcium-sensing receptors signal constitutive macropinocytosis and facilitate the uptake of NOD2 ligands in macrophages. *Nat. Commun.* **7**, 11284.

Chang, W.-T., Thomason, P. A., Gross, J. D. and Newell, P. C. (1998). Evidence that the RdeA protein is a component of a multistep phosphorelay modulating rate of development in *Dictyostelium*. *EMBO J.* **17**, 2809-2816.

Clark, J., Kay, R. R., Kielkowska, A., Niewczas, I., Fets, L., Oxley, D., Stephens, L. R. and Hawkins, P. T. (2014). *Dictyostelium* uses ether-linked inositol phospholipids for intracellular signalling. *EMBO J.* 33, 2188-2200.

Commisso, C., Davidson, S. M., Soydaner-Azeloglu, R. G., Parker, S. J., Kamphorst, J. J., Hackett, S., Grabocka, E., Nofal, M., Drebin, J. A., Thompson, C. B. et al. (2013). Macropinocytosis of protein is an amino acid supply route in Ras-transformed cells. *Nature* **497**, 633-637.

Commisso, C., Flinn, R. J. and Bar-Sagi, D. (2014). Determining the macropinocytic index of cells through a quantitative image-based assay. *Nat. Protoc.* **9**, 182-192.

Dumontier, M., Hocht, P., Mintert, U. and Faix, J. (2000). Rac1 GTPases control filopodia formation, cell motility, endocytosis, cytokinesis and development in *Dictyostelium*. *J. Cell Sci.* **113**, 2253-2265.

Falcon, B., Cavallini, A., Angers, R., Glover, S., Murray, T. K., Barnham, L., Jackson, S., O'neill, M. J., Isaacs, A. M., Hutton, M. L. et al. (2015). Conformation determines the seeding potencies of native and recombinant Tau aggregates. *J. Biol. Chem.* **290**, 1049-1065.

Fares, H. and Greenwald, I. (2001). Genetic analysis of endocytosis in *Caenorhabditis elegans*: coelomocyte uptake defective mutants. *Genetics* **159**, 133-145.

Fevrier, B., Vilette, D., Archer, F., Loew, D., Faigle, W., Vidal, M., Laude, H. and Raposo, G. (2004). Cells release prions in association with exosomes. *Proc. Natl. Acad. Sci. USA* **101**, 9683-9688.

Fey, P., Dodson, R. J., Basu, S. and Chisholm, R. L. (2013). One stop shop for everything *Dictyostelium*: dictyBase and the Dicty Stock Center in 2012. *Methods Mol. Biol.* **983**, 59-92.

Franke, J. and Kessin, R. (1977). A defined minimal medium for axenic strains of *Dictyostelium discoideum*. *Proc. Natl. Acad. Sci. USA* **74**, 2157-2161.

Glynn, P. J. and Clarke, K. R. (1984). An investigation of adhesion and detachment in slime mould amoebae using columns of hydrophobic beads. *Exp. Cell Res.* **152**, 117-126.

Hacker, U., Albrecht, R. and Maniak, M. (1997). Fluid-phase uptake by macropinocytosis in *Dictyostelium*. *J. Cell Sci.* **110**, 105-112.

Hadwiger, J. A. and Firtel, R. A. (1992). Analysis of Galpha4, a G-protein subunit required for multicellular development in *Dictyostelium*. *Genes Dev.* **6**, 38-49.

Hadwiger, J. A. and Srinivasan, J. (1999). Folic acid stimulation of the Galpha4 G protein-mediated signal transduction pathway inhibits anterior prestalk cell development in *Dictyostelium*. *Differentiation* **64**, 195-204.

Hardt, W. D., Chen, L. M., Schuebel, K. E., Bustelo, X. R. and Galan, J. E. (1998). *S. typhimurium* encodes an activator of Rho GTPases that induces membrane ruffling and nuclear responses in host cells. *Cell* 93, 815-826.

Harwood, A. J., Hopper, N. A., Simon, M.-N., Bouzid, S., Veron, M. and Williams, J. G. (1992). Multiple roles for cAMP-dependent protein kinase during *Dictyostelium* development. *Dev. Biol.* **149**, 90-99.

Hoeller, O., Bolourani, P., Clark, J., Stephens, L. R., Hawkins, P. T., Weiner, O. D., Weeks, G. and Kay, R. R. (2013). Two distinct functions for PI3-kinases in macropinocytosis. *J. Cell Sci.* **126**, 4296-4307.

Junemann, A., Filić, V., Winterhoff, M., Nordholz, B., Litschko, C., Schwellenbach, H., Stephan, T., Weber, I. and Faix, J. (2016). A Diaphanous-related formin links Ras signaling directly to actin assembly in macropinocytosis and phagocytosis. *Proc. Natl. Acad. Sci. USA* **113**, E7464-E7473.

Katoh, M., Chen, G., Roberge, E., Shaulsky, G. and Kuspa, A. (2007). Developmental commitment in *Dictyostelium discoideum*. *Eukaryot. Cell* **6**, 2038-2045.

Kay, R. R. (1989). Evidence that elevated intracellular cyclic AMP triggers spore maturation in *Dictyostelium*. *Development* **105**, 753-759.

Kayman, S. C. and Clarke, M. (1983). Relationship between axenic growth of *Dictyostelium discoideum* strains and their track morphology on substrates coated with gold particles. *J. Cell Biol.* **97**, 1001-1010.

Khosla, M., Splegelman, G. B. and Weeks, G. (2005). The effect of the disruption of a gene encoding a PI4 kinase on the developmental defect exhibited by *Dictyostelium* rasC− cells. *Dev. Biol.* **284**, 412-420.

King, J. S., Veltman, D. M. and Insall, R. H. (2011). The induction of autophagy by mechanical stress. *Autophagy* **7**, 1490-1499.

Koivusalo, M., Welch, C., Hayashi, H., Scott, C. C., Kim, M., Alexander, T., Touret, N., Hahn, K. M. and Grinstein, S. (2010). Amiloride inhibits macropinocytosis by lowering submembranous pH and preventing Rac1 and Cdc42 signaling. *J. Cell Biol.* **188**, 547-563.

Langridge, P. D. and Kay, R. R. (2007). Mutants in the *Dictyostelium* Arp2/3 complex and chemoattractant-induced actin polymerization. *Exp. Cell Res.* **313**, 2563-2574.

Lee, S., Comer, F. I., Sasaki, A., Mcleod, I. X., Duong, Y., Okumura, K., Yates, J. R., Parent, C. A. and Firtel, R. A. (2005). TOR complex 2 integrates cell movement during chemotaxis and signal relay in *Dictyostelium*. *Mol. Biol. Cell* **16**, 4572-4583.

Lewis, W. H. (1931). Pinocytosis. *Johns Hopkins Hosp. Bull.* **49**, 17-27.

Lewis, W. H. (1937). Pinocytosis by malignant cells. *Cancer Res.* **29**, 666-679.

Ludlow, M. J., Traynor, D., Fisher, P. R. and Ennion, S. J. (2008). Purinergic-mediated Ca2+ influx in Dictyostelium discoideum. *Cell Calcium* **44**, 567-579.

Lukyanenko, V., Malyukova, I., Hubbard, A., Delannoy, M., Boedeker, E., Zhu, C., Cebotaru, L. and Kovbasnjuk, O. (2011). Enterohemorrhagic *Escherichia coli* infection stimulates Shiga toxin 1 macropinocytosis and transcytosis across intestinal epithelial cells. *Am. J. Physiol. Cell Physiol.* **301**, C1140-C1149.

Maeda, Y. (1983). Axenic growth of *Dictyostelium discoideum* wild-type NC-4 cells and its relation to endocytotic ability. *J. Gen. Microbiol.* **129**, 2467-2473.

Maeda, Y. (1988). Changes of endocytotic activities during the cell cycle of *Dictyostelium* cells. *Dev. Growth Differ.* **30**, 15-24.

Maeda, Y. and Kawamoto, T. (1986). Pinocytosis in *Dictyostelium discoideum* cells: a possible implication of cytoskeletal actin for pinocytotic activity. *Exp. Cell Res.* **164**, 516-526.

Magzoub, M., Sandgren, S., Lundberg, P., Oglecka, K., Lilja, J., Wittrup, A., Göran Eriksson, L. E., Langel, Ü., Belting, M. and Gräslund, A. (2006). N-terminal peptides from unprocessed prion proteins enter cells by macropinocytosis. *Biochem. Biophys. Res. Commun.* **348**, 379-385.

Mann, S. K. O. and Firtel, R. A. (1991). A developmentally regulated, putative serine/threonine protein kinase is essential for development in *Dictyostelium*. *Mech. Dev.* **35**, 89-101.

Marechal, V., Prevost, M.-C., Petit, C., Perret, E., Heard, J.-M. and Schwartz, O. (2001). Human immunodeficiency virus type 1 entry into macrophages mediated by macropinocytosis. *J. Virol.* **75**, 11166-11177.

Marin, F. T. (1976). Regulation of development in *Dictyostelium discoideum*: I. Initiation of the growth to development transition by amino acid starvation. *Dev. Biol.* **48**, 110-117.

Meena, N. P. and Kimmel, A. R. (2017). Chemotactic network responses to live bacteria show independence of phagocytosis from chemoreceptor sensing. *eLife* **6**, e24627.

Morris, H. R., Taylor, G. W., Masento, M. S., Jermyn, K. A. and Kay, R. R. (1987). Chemical structure of the morphogen differentiation inducing factor from Dictyostelium discoideum. *Nature* **328**, 811-814.

Morris, H. R., Masento, M. S., Taylor, G. W., Jermyn, K. A. and Kay, R. R. (1988). Structure elucidation of two differentiation inducing factors (DIF-2 and DIF-3) from the cellular slime mould Dictyostelium discoideum. *Biochem. J.* **249**, 903-906.

Münch, C., O'brien, J. and Bertolotti, A. (2011). Prion-like propagation of mutant superoxide dismutase-1 misfolding in neuronal cells. *Proc. Natl. Acad. Sci. USA* **108**, 3548-3553.

Nanbo, A., Imai, M., Watanabe, S., Noda, T., Takahashi, K., Neumann, G., Halfmann, P. and Kawaoka, Y. (2010). *Ebolavirus* is internalized into host cells via macropinocytosis in a viral glycoprotein-dependent manner. *PLoS Pathog.* 6, e1001121.

Norbury, C. C., Hewlett, L. J., Prescott, A. R., Shastri, N. and Watts, C. (1995). Class I MHC presentation of exogenous soluble antigen via macropinocytosis in bone marrow macrophages. *Immunity* **3**, 783-791.

Novak, K. D., Peterson, M. D., Reedy, M. C. and Titus, M. A. (1995). *Dictyostelium* myosin I double mutants exhibit conditional defects in pinocytosis. *J. Cell Biol.* 131, 1205-1221.

O'halloran, T. J. and Anderson, R. G. W. (1992). Clathrin heavy chain is required for pinocytosis, the presence of large vacuoles, and development in *Dictyostelium*. *J. Cell Biol.* **118**, 1371-1377.

Pan, M., Xu, X., Chen, Y. and Jin, T. (2016). Identification of a chemoattractant G-protein-coupled receptor for folic acid that controls both chemotaxis and phagocytosis. *Dev. Cell* **36**, 428-439.

Parent, C. A., Blacklock, B. J., Froehlich, W. M., Murphy, D. B. and Devreotes, P. N. (1998). G Protein signaling events are activated at the leading edge of chemotactic cells. *Cell* **95**, 81-91.

Patel, H. and Barber, D. L. (2005). A developmentally regulated Na-H exchanger in *Dictyostelium discoideum* is necessary for cell polarity during chemotaxis. *J. Cell Biol.* **169**, 321-329.

Pintsch, T., Satre, M., Klein, G., Martin, J.-B. and Schuster, S. C. (2001). Cytosolic acidification as a signal mediating hyperosmotic stress responses in *Dictyostelium discoideum*. *BMC Cell Biol.* **2**, 9.

Primpke, G., Iassonidou, V., Nellen, W. and Wetterauer, B. (2000). Role of cAMP-dependent protein kinase during growth and early development of *Dictyostelium discoideum*. *Dev. Biol.* **221**, 101-111.

Rai, A., Pathak, D., Thakur, S., Singh, S., Dubey, A. K. and Mallik, R. (2016). Dynein clusters into lipid microdomains on phagosomes to drive rapid transport toward lysosomes. *Cell* **164**, 722-734.

Rivero, F. and Maniak, M. (2006). Quantitative and microscopic methods for studying the endocytic pathway. *Methods Mol. Biol.* **346**, 423-438.

Rodriguez, M., Kim, B., Lee, N.-S., Veeranki, S. and Kim, L. (2008). MPL1, a novel phosphatase with leucine-rich repeats, is essential for proper ERK2 phosphorylation and cell motility. *Euk. Cell* **7**, 958-966.

Rosel, D., Khurana, T., Majithia, A., Huang, X., Bhandari, R. and Kimmel, A. R. (2012). TOR complex 2 (TORC2) in *Dictyostelium* suppresses phagocytic nutrient capture independently of TORC1-mediated nutrient sensing. *J. Cell Sci.* **125**, 37-48.

Saito, T., Taylor, G. W., Yang, J.-C., Neuhaus, D., Stetsenko, D., Kato, A. and Kay, R. R. (2006). Identification of new differentiation inducing factors from *Dictyostelium discoideum*. *Biochim. Biophys. Acta* **1760**, 754-761.

Sallusto, F., Cella, M., Danieli, C. and Lanzavecchia, A. (1995). Dendritic cells use macropinocytosis and the mannose receptor to concentrate macromolecules in the major histocompatibility complex class II compartment: downregulation by cytokines and bacterial products. *J. Exp. Med.* **182**, 389-400.

Sancak, Y., Bar-Peled, L., Zoncu, R., Markhard, A. L., Nada, S. and Sabatini, D. M. (2010). Ragulator-Rag complex targets mTORC1 to the lysosomal surface and is necessary for its activation by amino acids. *Cell* **141**, 290-303.

Sattler, N., Monroy, R. and Soldati, T. (2013). Quantitative analysis of phagocytosis and phagosome maturation. *Methods Mol. Biol.* **983**, 383-402.

Scavello, M., Petlick, A. R., Ramesh, R., Thompson, V. F., Lotfi, P. and Charest, P. G. (2017). Protein kinase A regulates the Ras, Rap1 and TORC2 pathways in response to the chemoattractant cAMP in *Dictyostelium*. *J. Cell Sci.* **130**, 1545-1558.

Shaulsky, G., Fuller, D. and Loomis, W. F. (1998). A cAMP-phosphodiesterase controls PKA-dependent differentiation. *Development* **125**, 691-699.

Shu, S., Liu, X. and Korn, E. D. (2005). Blebbistatin and blebbistatin-inactivated myosin II inhibit myosin II-independent processes in *Dictyostelium*. *Proc. Natl. Acad. Sci. USA* **102**, 1472-1477.

Shutes, A., Onesto, C., Picard, V., Leblond, B., Schweighoffer, F. and Der, C. J. (2007). Specificity and mechanism of action of EHT 1864, a novel small molecule inhibitor of Rac family small GTPases. *J. Biol. Chem.* **282**, 35666-35678.

Suess, P. M. and Gomer, R. H. (2016). Extracellular polyphosphate inhibits proliferation in an autocrine negative feedback loop in *Dictyostelium discoideum*. *J. Biol. Chem.* **291**, 20260-20269.

Swanson, J. A. (2008). Shaping cups into phagosomes and macropinosomes. *Nat. Rev. Mol. Cell Biol.* **9**, 639-649.

Taniura, H., Sanada, N., Kuramoto, N. and Yoneda, Y. (2006). A metabotropic glutamate receptor family gene in *Dictyostelium discoideum*. *J. Biol. Chem.* **281**, 12336-12343.

Tekinay, T., Wu, M. Y., Otto, G. P., Anderson, O. R. and Kessin, R. H. (2006). Function of the *Dictyostelium discoideum* atg1 kinase during autophagy and development. *Euk. Cell* **5**, 1797-1806.

Thilo, L. and Vogel, G. (1980). Kinetics of membrane internalization and recycling during pinocytosis in *Dictyostelium discoideum*. *Proc. Natl. Acad. Sci. USA* **77**, 1015-1019.

Thomason, P. A., Traynor, D., Cavet, G., Chang, W.-T., Harwood, A. J. and Kay, R. R. (1998). An intersection of the cAMP/PKA and two-component signal transduction systems in *Dictyostelium*. *EMBO J.* **17**, 2838-2845.

Thomason, P. A., Traynor, D., Stock, J. B. and Kay, R. R. (1999). The RdeA-RegA system, a eukaryotic phospho-relay controlling cAMP breakdown. *J. Biol. Chem.* **274**, 27379-27384.

Thoreen, C. C. and Sabatini, D. M. (2009). Rapamycin inhibits mTORC1, but not completely. *Autophagy* **5**, 725-726.

Traynor, D. and Kay, R. R. (2007). Possible roles of the endocytic cycle in cell motility. *J. Cell Sci.* **120**, 2318-2327.

Traynor, D. and Kay, R. R. (2017). A polycystin-type transient receptor potential (Trp) channel that is activated by ATP. *Biol Open* **6**, 200-209.

Veltman, D. M. (2015). Drink or drive: competition between macropinocytosis and cell migration. *Biochem. Soc. Trans.* **43**, 129-132.

Veltman, D. M., Williams, T. D., Bloomfield, G., Chen, B.-C., Betzig, E., Insall, R. H. and Kay, R. R. (2016). A plasma membrane template for macropinocytic cups. *eLife* **5**, e20085.

Watts, D. J. and Ashworth, J. M. (1970). Growth of myxamoebae of the cellular slime mould *Dictyostelium discoideum* in axenic culture. *Biochem. J.* **119**, 171-174.

Wu, L. J., Valkema, R., Van Haastert, P. J. M. and Devreotes, P. N. (1995). The G protein beta subunit is essential for multiple responses to chemoattractants in *Dictyostelium*. *J. Cell Biol.* **129**, 1667-1675.

Yoshida, S., Pacitto, R., Yao, Y., Inoki, K. and Swanson, J. A. (2015). Growth factor signaling to mTORC1 by amino acid-laden macropinosomes. *J. Cell Biol.* **211**, 159-172.

Supplemental Information

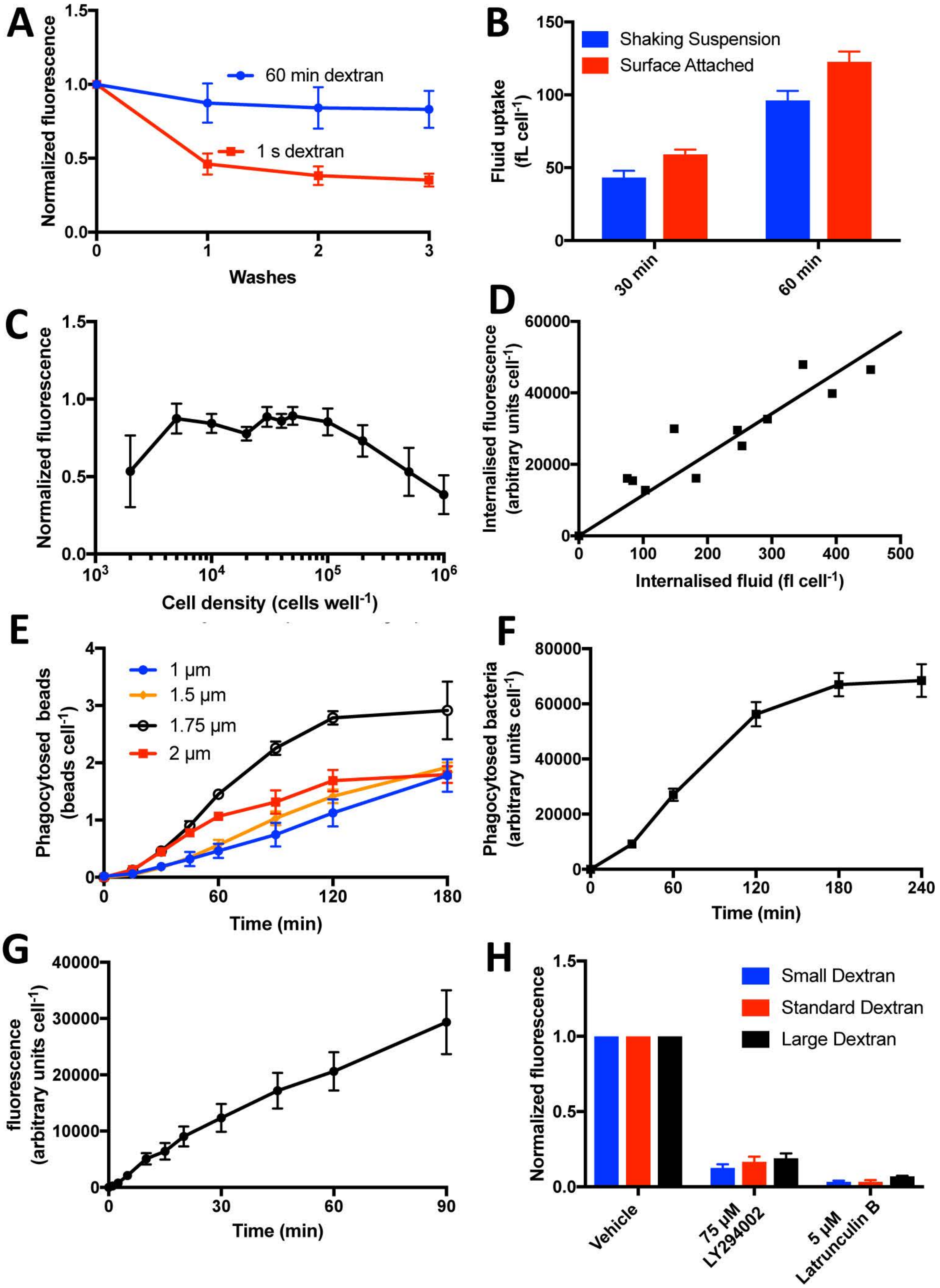

Figure S1: Fluid and other uptake measurements by flow cytometry

A) One wash is sufficient to remove most TRITC-dextran bound to the surface of cells. Ax2 cells in 96-well plates were loaded with TRITC-dextran for either 60 minutes (average 0-wash fluorescence 11670) or 1 second (average 0-wash fluorescence 695), the media thrown off, the cells washed *in-situ* with ice-cold KK_2MC and cellular fluorescence quantified by flow cytometry (n=4). Fluorescence was normalised to that of unwashed cells from the same condition. **B)** Fluid uptake by Ax2 cells is similar whether they are on a surface, as in the high-throughput assay, or in the more standard shaking suspension. Uptake was measured by flow cytometry. **C)** Cell density affects the rate of fluid uptake. Axenically grown Ax2 cells were spun down by centrifugation and resuspended to various densities in HL5. 50 µl of cells were added to triplicate wells of a 96-well plate and allowed to settle for one hour. TRITC-dextran was added for one hour after which internalised fluorescence was measured and normalised to the cell concentration giving maximum fluid uptake that day; 5000 to 50,000 cells per well gave very similar results. **D)** Calibration curve for converting flow cytometry fluorescence values to fluid uptake volumes. Cells in shaking suspension were fed TRITC-dextran for various times on 4 different days and their internalised fluorescence was determined by both fluorimetry and flow cytometry. Absolute volumes of uptake were determined from the fluorimetric measurements and used to construct a calibration curve for the flow cytometry measurements (since cells measured in both ways have taken up the same volumes). **E)** Phagocytosis of beads by Ax2 cells grown in HL5 measured by flow cytometry using the bead concentrations indicated in the materials and methods. The small lag in uptake after adding beads is likely due to the beads settling onto the cells, which increases their effective concentration. Differences in the rate of settling means that uptake of different sized beads should not be directly compared using this assay. **F)** Uptake of Texas-red *E. coli* bioparticles by axenically growing Ax2 cells measured using high-throughput flow cytometry. The uptake dynamics are similar to those for bead uptake. **G)** Membrane uptake dynamics measured using FM1-43 dye (n=4). These are similar to those previously published (Aguado-Velasco and Bretscher, 1999), with the highest rate of membrane uptake within the first 10 minutes. **H)** Fluid uptake is similar with different sized dextrans. Fluid uptake was measured using small (4,400 MW), standard (155,000 MW) and large (500,000 MW) TRITC-dextran as the fluid phase marker. Inhibition of fluid uptake was similar with each dextran when either the PI3K inhibitor LY294002 or the actin inhibitor Latrunculin B were used, indicating that macropinocytosis is responsible for the overwhelming majority of fluid uptake by axenically growing *Dictyostelium*. Error bars show the s.e.m.; n=3 unless otherwise stated.

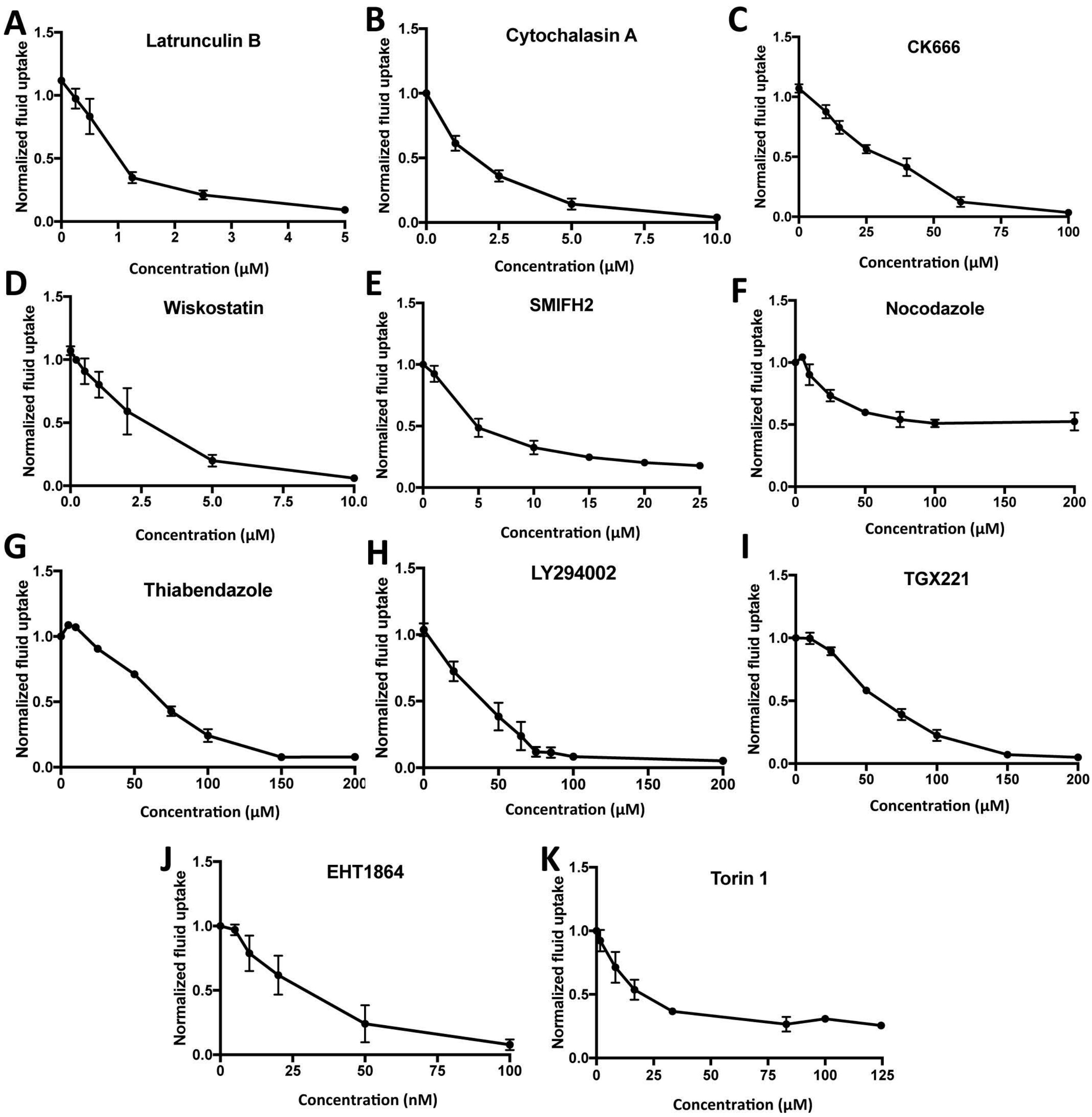

Figure S2: Inhibitor dose response curves

Dose response curves were determined for compounds from table 1 that inhibited macropinocytosis. Fluid uptake by Ax2 cells grown in HL5 was measured for the hour after the addition of each inhibitor, and normalised to treatment with vehicle alone. **A)** Latrunculin B **B)** Cytochalasin A **C)** CK666 **D)** Wiskostatin **E)** SMIFH2 **F)** Nocodazole **G)** Thiabendazole **H)** LY294002 **I)** TGX221 **J)** EHT1864 **K)** Torin 1. The error bars shown are the s.e.m.; n=3.

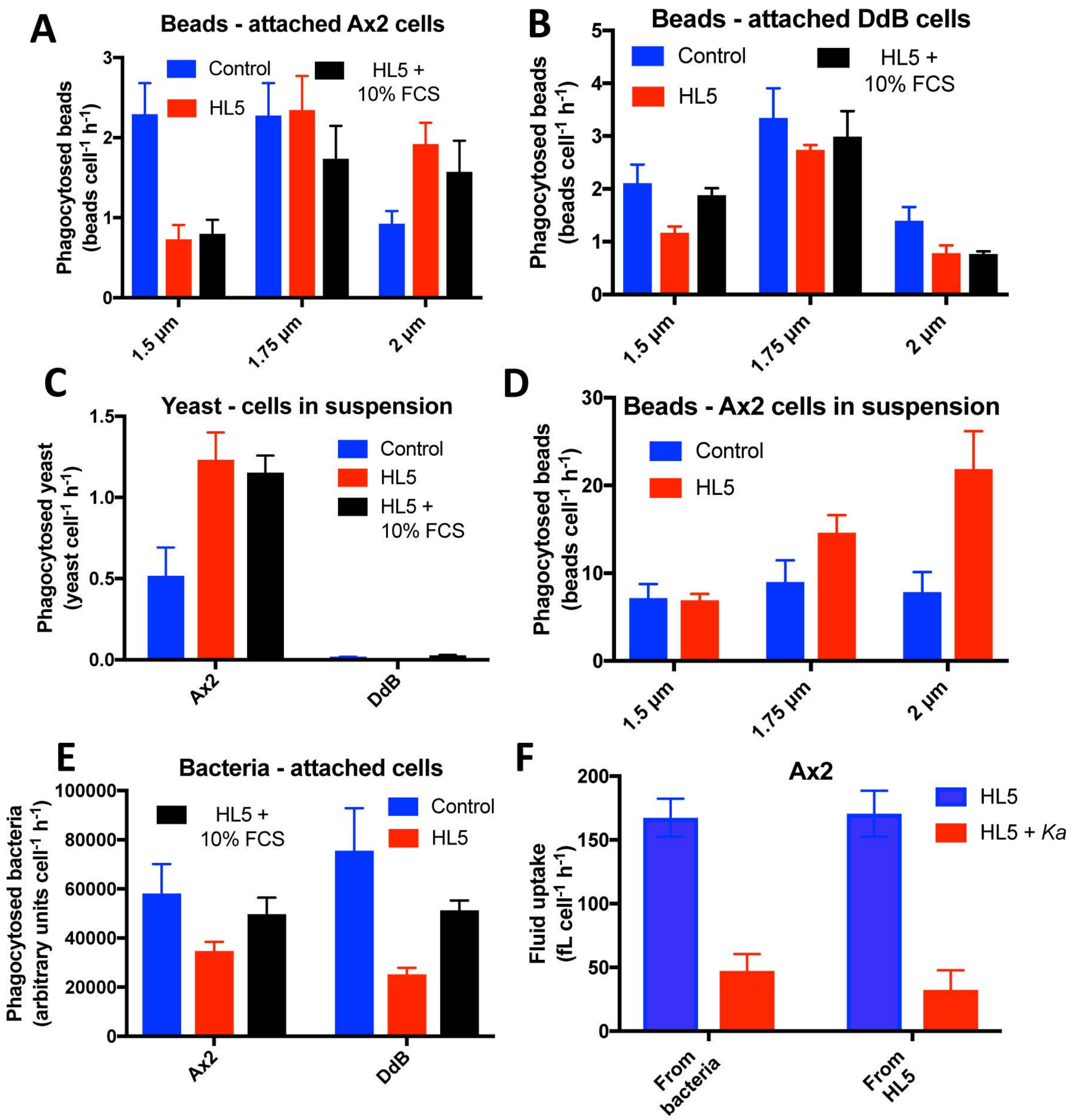

Figure S3: Phagocytosis of large particles correlates with increased size of macropinosomes; and phagocytosis is the preferred feeding mode for cells presented with both bacteria and liquid medium.

A) The increased rates of macropinocytosis and larger macropinosomes (see

Figure 2C&D) of Ax2 cells grown in liquid media correlates with an increased ability to take up large particles. The uptake of various sizes of beads by Ax2 cells adapted to the indicated conditions is compared (n=3). Cells growing on bacteria take up 1.5 µm beads better than those from HL5 (p=0.02, unpaired t-test), but this is reversed for 2 µm beads (p=0.03, unpaired t-test). **B)** The increased rate of macropinocytosis in DdB cells grown in HL5+10% FCS, which does not result in larger macropinosomes (Figure 2F), does not result in increased uptake of large particles. DdB cells adapted to the indicated conditions are compared. As phagocytosis of beads by cells attached to a surface is limited by the availability of beads, we tested cells in shaking suspension with an excess of particles. **C)** Phagocytosis of yeast by Ax2 is increased when the cells are incubated in growth media beforehand (p=0.04 for control compared to HL5, unpaired t-test), whereas DdB cells do not take up yeast under any of the conditions tested (n=3). **D)** Phagocytosis of larger beads by Ax taken from growth medium was higher than that of Ax2 cells taken from bacteria (p<0.05 for 2µm beads, unpaired t-test). Uptake was in shaking suspension with a large excess of particles (n=3). **E)** The uptake of small, bacteria-sized particles is not increased in Ax2 cells with high macropinocytosis rates; if anything the reverse. The uptake of Texas-red *E. coli* bioparticles is compared in cells adapted to the indicated conditions (n=3). **F)** The addition of bacteria to Ax2 cells growing in HL5 medium results in a downregulation of macropinocytosis indicating that phagocytosis is the preferred feeding mode in these conditions (n=6, p<0.0001 for cells from bacteria and 0.0006 for cells from HL5 in unpaired t-tests). Control indicates cells grown on bacteria, for the other conditions cells were harvested and incubated for 24 hours in the indicated medium, except in D where the 'HL5' cells were taken from logarithmic growth in HL5 in shaking suspension. Error bars show the s.e.m.

Journal of Cell Science • Supplementary information

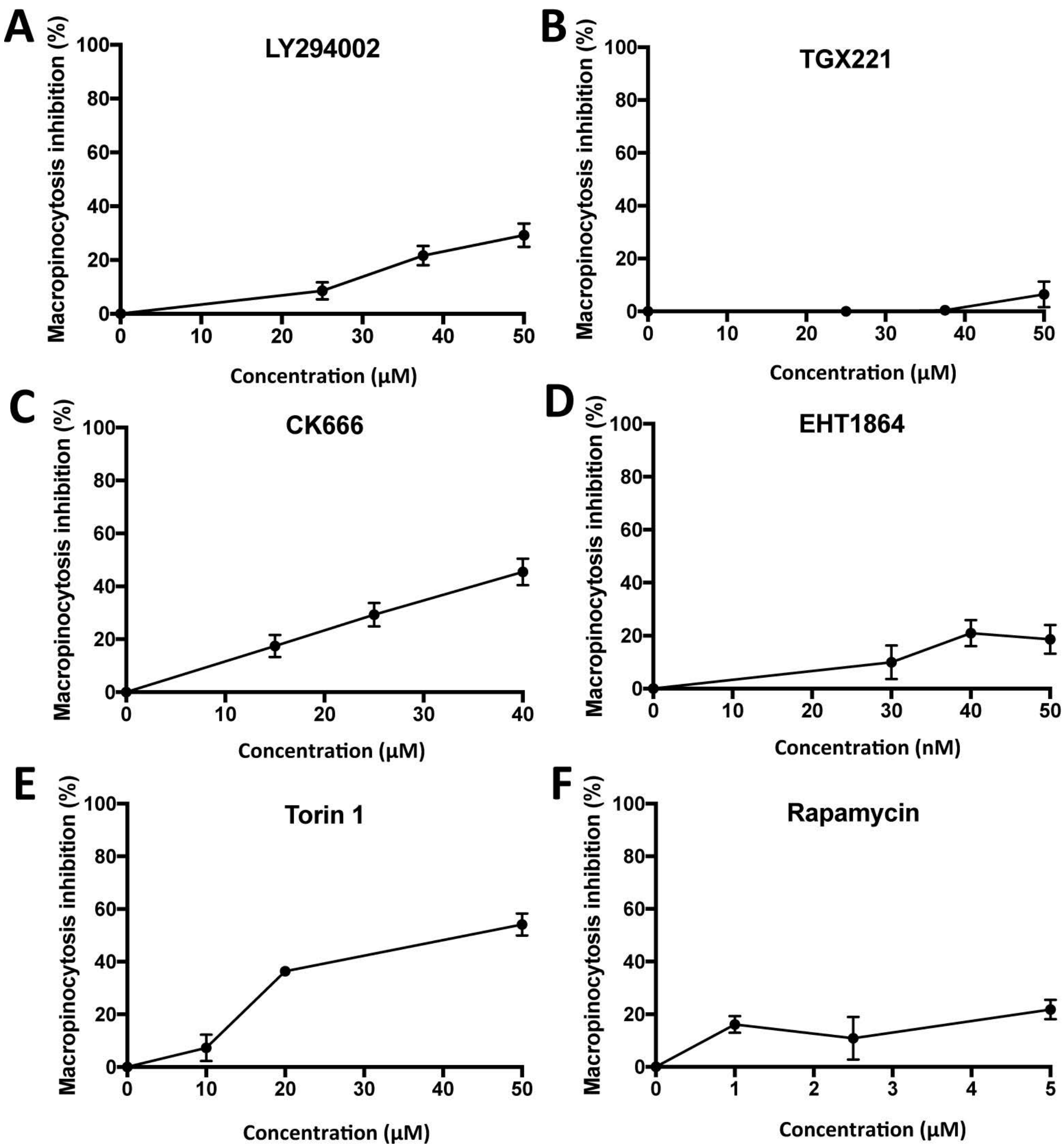

Figure S4: Recovery of cells from long-term inhibitor treatment

To obtain correction factors for Figure 4, Ax2 cells growing in HL5 in 96-well plates were treated with **(A)** LY294002, n=3, **(B)** TGX221, n=4, **(C)** CK666, n=4, **(D)** EHT1864, n=4, **(E)** torin 1, n=3, and **(F)** rapamycin, n=3, for 10 hours. The drugs were washed away by dunk-banging, the cells allowed to recover in HL5 for 10 minutes before fluid uptake was measured over 1 hour using the high-throughput flow cytometry assay. Fluid uptake by treated cells was compared to that by those treated with vehicle to calculate the percentage inhibition of macropinocytosis.

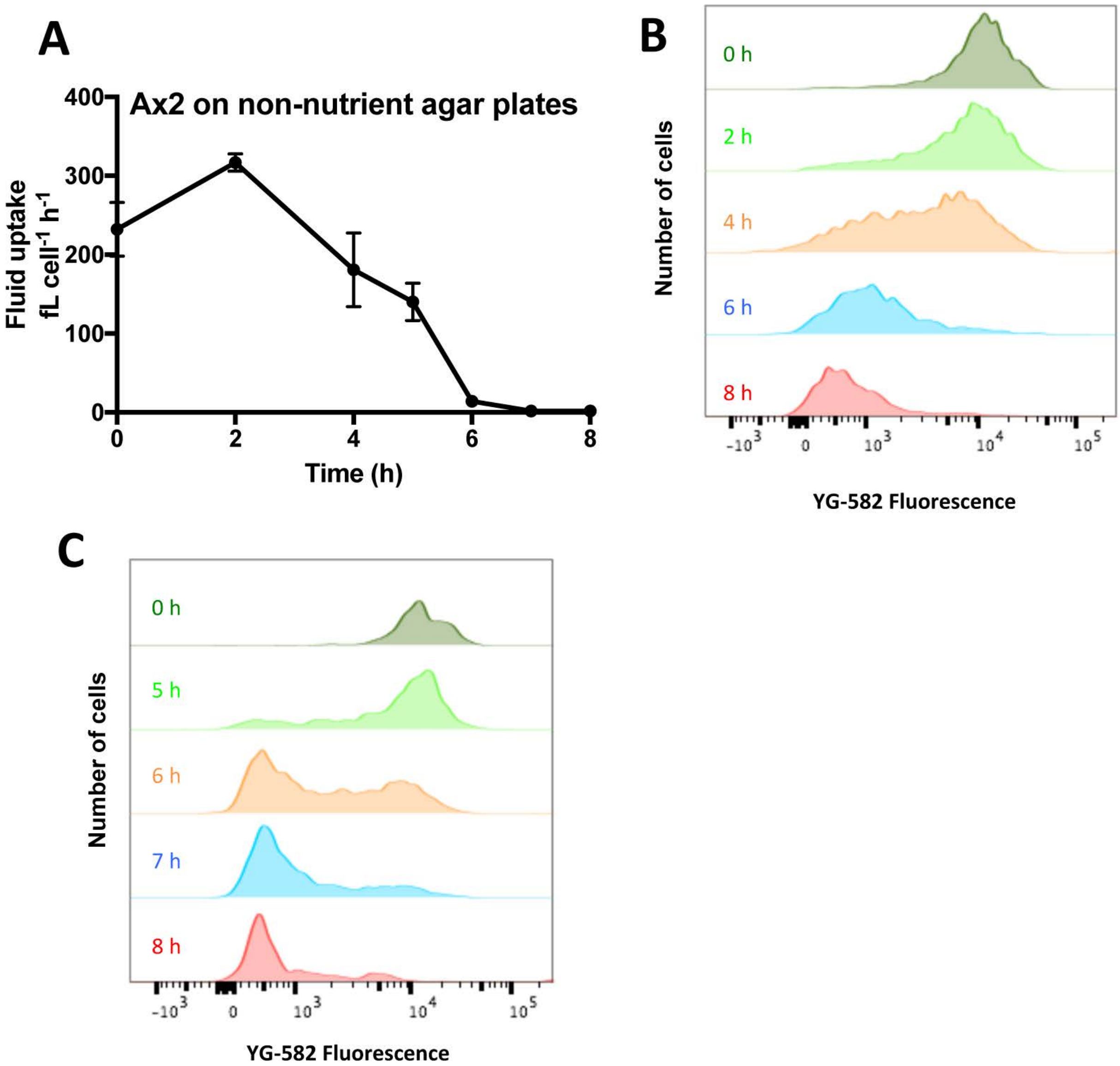

Figure S5: Downregulation of macropinocytosis during development

A) Ax2 cells grown in HL5 (high macropinocytosis) were washed free of nutrients, developed on non-nutrient agar and their fluid uptake in one hour measured over time (n=4). **B)** Representative histograms showing the fluid uptake of cell populations over time during development induced by cyclic-AMP pulsing. **C)** Representative histograms showing the fluid uptake of cell populations over time during development on non-nutrient agar. In both standard development assays, cells switch macropinocytosis off prior to forming tight aggregates.

Journal of Cell Science • Supplementary information

Table S1: Induction of macropinocytosis by individual amino acids

Only arginine, glutamate and lysine can individually induce upregulation of macropinocytosis of 2-fold or greater at the concentrations tested. Ax2 cells, harvested from bacterial plates, were incubated for 24 hours with all 20 common L-amino acids in KK_2MC, pH 6.2 at the concentrations indicated, and fluid uptake then measured using the high-throughput flow cytometry assay (N/A indicates that no result was obtained due to solubility problems of the amino acid in this buffer). Results are given relative to the control without amino acids; s.e.m. is shown in brackets; n=3.

	Normalized fluid uptake (s.e.m.)				
Amino acid / Concentration	0 mM	5 mM	10 mM	20 mM	50 mM
Alanine	1	0.74 (0.08)	0.86 (0.11)	1.09 (0.29)	0.97 (0.10)
Arginine	1	0.80 (0.09)	0.83 (0.11)	1.04 (0.11)	2.88 (0.72)
Cysteine	1	1.29 (0.20)	1.26 (0.38)	0.69 (0.24)	N/A
Glycine	1	0.82 (0.26)	0.62 (0.13)	0.65 (0.16)	0.70 (0.15)
Lysine	1	0.94 (0.14)	1.46 (0.38)	2.49 (0.96)	6.66 (2.18)
Proline	1	1.12 (0.30)	0.69 (0.09)	0.83 (0.13)	0.83 (0.08)
Threonine	1	0.95 (0.23)	1.06 (0.20)	0.79 (0.09)	0.75 (0.26)
Serine	1	0.65 (0.19)	0.46 (0.29)	0.68 (0.29)	0.95 (0.49)
Histidine	1	1.16 (0.66)	0.64 (0.20)	0.75 (0.19)	0.62 (0.10)
Valine	1	0.82 (0.30)	0.97 (0.41)	0.82 (0.38)	0.91 (0.41)
Glutamine	1	0.67 (0.28)	0.74 (0.47)	1.10 (0.56)	0.99 (0.37)
Isoleucine	1	0.41 (0.18)	0.53 (0.23)	0.58 (0.26)	0.68 (0.33)
Leucine	1	0.70 (0.07)	0.65 (0.24)	0.71 (0.24)	0.69 (0.21)
Methionine	1	0.66 (0.13)	0.59 (0.19)	0.67 (0.10)	0.73 (0.10)
Asparagine	1	1.08 (0.52)	0.84 (0.15)	0.94 (0.09)	0.90 (0.10)
Aspartate	1	0.76 (0.16)	0.55 (0.09)	0.77 (0.18)	1.00 (0.30)
Glutamate	1	0.76 (0.32)	0.84 (0.30)	1.58 (0.49)	6.88 (2.89)
Phenylalanine	1	0.78 (0.09)	0.73 (0.07)	0.80 (0.12)	0.91 (0.29)
Tryptophan	1	0.73 (0.14)	0.62 (0.08)	0.62 (0.17)	0.51 (0.07)
Tyrosine	1	0.89 (0.24)	N/A	N/A	N/A

Table S2: Only metabolisable sugars induce macropinocytosis

Only sugars known to be metabolisable by *Dictyostelium* (Ashworth and Watts, 1970, Watts and Ashworth, 1970) induce upregulation of macropinocytosis (glucose, fructose, mannose, maltose all induced a ~2-fold increase or greater compared to the control). This suggests that sugars are sensed by their effect on metabolism, perhaps through downstream sensing based on a common metabolite. Ax2 cells, harvested from bacterial plates, were incubated with the individual sugars for 24 hours, and fluid uptake then measured using the high-throughput flow cytometry assay. Monosaccharides were dissolved at 55 mM (the glucose concentration in SIH) and in addition, sugars with more than one saccharide unit were tested at concentrations to obtain equivalent numbers of saccharides in the media. Each experiment was repeated at least three times, with three replicates a time; s.e.m. is shown in brackets; n=6.

Sugar	**Concentration (mM)**	**Metabolisable by *Dictyostelium*?**	**Fold increase in macropinocytosis over buffer alone (s.e.m.)**
None	0	N/A	1 (0)
Glucose	55	Yes	3.83 (0.38)
Galactose	55	No	1.17 (0.15)
Fructose	55	Poorly	2.34 (0.46)
Sorbitol	55	No	1.16 (0.21)
Mannose	55	Yes	4.09 (0.67)
Maltose	55 / 27.5	Yes	2.22 (0.31) / 4.00 (0.66)
Sucrose	55 / 27.5	No	1.48 (0.13) / 1.54 (0.15)
Raffinose	55 / 18.3	?	2.49 (0.40) / 2.86 (0.62)

Journal of Cell Science • Supplementary information

Table S3: Developmental signals tested for the ability to induce downregulation of macropinocytosis in non-nutrient conditions

Various compounds involved in *Dictyostelium* development were tested for the ability to induce downregulation of macropinocytosis by low-density starving cells, although none did. Axenically growing Ax2 cells in a 96-well plate were washed twice by dunk-banging in KK_2MC and incubated for 17 hours in KK_2MC containing the compounds at various concentrations (n=3). The effect of the compound on downregulation of Ax2 macropinocytosis was ascertained by comparing the fluid uptake of cells treated with the compound to those in KK_2MC without any compound.

Media addition Tested	Maximum concentration tested	Induced downregulation of macropinocytosis?
cyclic-AMP	10 mM	No
Non-hydrolysable cyclic-AMP	10 mM	No
Non-hydrolysable ATP	100 µM	No
Adenosine	500 µM	No
DIF-1	100 nM	No
DIF-2	100 nM	No
MPBD	100 nM	No
Polyphosphate	200 µM	No

Journal of Cell Science • Supplementary information

Table S4: Strains used in this work

A list of the strains used in this work, and where they were obtained.

Strain	Parent	Source	Strain ID
DdB	NC4	D Welker	N/A
Ax2-Ka	DdB	R R Kay	N/A
fAR1-	Ax2	Pan et al., 2016	DBS0350717
gpbA-	Ax2-MRC	P Devreotes	HM1691
gpaD-	JH8	Hadwiger and Firtel, 1992	JH417
erkB-	Ax2-MRC	Nichols et al., in preparation	HM1735
pkaC-	Ax2	Primpke et al., 2000	HM1037
regA-	Ax2-MRC	Thomason et al., 1998	HM1015
rdeA-	Ax2	Chang et al., 1998	WTC10-H2